MARTIN MARIETTA ENERGY SYSTEMS LIBRARIES

3 4456 0353284 4

ORNL/TM-12070
(CESAR-92/09)

OAK RIDGE NATIONAL LABORATORY

MARTIN MARIETTA

Time Optimal Trajectories f Mobile Robots with Two Independently Driven Whee

David B. Reister
François G. Pin

OAK RIDGE NATIONAL LABORATORY
CENTRAL RESEARCH LIBRARY
CIRCULATION SECTION
4500N ROOM 175
LIBRARY LOAN COPY
DO NOT TRANSFER TO ANOTHER PERSON
If you wish someone else to see this report, send in name with report and the library will arrange a loan.
(NON-RECORD)

MANAGED BY
MARTIN MARIETTA ENERGY SYSTEMS, INC.
FOR THE UNITED STATES
DEPARTMENT OF ENERGY

This report has been reproduced directly from the best available copy.

Available to DOE and DOE contractors from the Office of Scientific and Technical Information, P.O. Box 62, Oak Ridge, TN 37831; prices available from (615) 576-8401, FTS 626-8401.

Available to the public from the National Technical Information Service, U.S. Department of Commerce, 5285 Port Royal Rd., Springfield, VA 22161.

This report was prepared as an account of work sponsored by an agency of the United States Government. Neither the United States Government nor any agency thereof, nor any of their employees, makes any warranty, express or implied, or assumes any legal liability or responsibility for the accuracy, completeness, or usefulness of any information, apparatus, product, or process disclosed, or represents that its use would not infringe privately owned rights. Reference herein to any specific commercial product, process, or service by trade name, trademark, manufacturer, or otherwise, does not necessarily constitute or imply its endorsement, recommendation, or favoring by the United States Government or any agency thereof. The views and opinions of authors expressed herein do not necessarily state or reflect those of the United States Government or any agency thereof.

ORNL/TM-12070
CESAR-92/09

Engineering Physics and Mathematics Division

TIME OPTIMAL TRAJECTORIES FOR MOBILE ROBOTS WITH TWO INDEPENDENTLY DRIVEN WHEELS

David B. Reister and François G. Pin

DATE PUBLISHED — March 1992

Research sponsored by the
Engineering Research Program
Office of Basic Energy Sciences
U.S. Department of Energy

Prepared by the
OAK RIDGE NATIONAL LABORATORY
Oak Ridge, Tennessee 37831
managed by
MARTIN MARIETTA ENERGY SYSTEMS, INC.
for the
U.S. DEPARTMENT OF ENERGY
under contract DE-AC05-84OR2140

MARTIN MARIETTA ENERGY SYSTEMS LIBRARIES

3 4456 0353284 4

CONTENTS

ABSTRACT vii
1. INTRODUCTION 1
2. KINEMATIC EQUATIONS OF MOTION FOR THE PLATFORM . . 3
3. THE GENERAL FORM OF THE OPTIMAL CONTROLS 5
4. PARAMETERIZATION OF THE BANG-BANG TRAJECTORIES . . 11
4.1 ANALYTICAL RELATIONSHIP BETWEEN THE SEGMENTS AND THE FINAL ORIENTATION 13
4.2 CALCULATION OF THE DUAL VARIABLES 14
5. BANG-BANG TRAJECTORIES 17
5.1 TRAJECTORIES TO A POINT 17
5.2 TRAJECTORIES TO A CONFIGURATION 20
6. OPTIMAL TRAJECTORIES 27
7. USE OF THE METHOD FOR ROBOT TRAJECTORY PLANNING . 35
8. CONCLUSIONS 37
REFERENCES 39

LIST OF FIGURES

Fig.		Page
1	The configuration of the platform is defined by the position (x, y) and orientation (ϕ)	4
2	Points that can be reached by trajectories with three switch times for a constant value of $T = \sqrt{10}$ sec	18
3	Curves showing the location of the furthest points in the first quadrant that can be reached by trajectories with three switch times for several values of T $(T^2 = 2, 4, 6, 8,$ and $10)$	19
4	Curve showing the ratio of τ^m and T. The sets (τ^m, T) define the intersection of the first arcs with the y axis	19
5	Cartesian paths of the robot for three-switch-time trajectories ending on the first arc defined by $T^2 = 10$	20
6	Points that can be reached by trajectories with four switch times for a constant value of $T(T^2 = 10)$ when the final orientation is 0.8 radians	21
7	Points that can be reached by trajectories with four switch times for a constant value of $T(T^2 = 10)$ when the final orientation is 1.57 radians	22
8	Points that can be reached by trajectories with four switch times for a constant value of $T(T^2 = 10)$ when the final orientation is 3.14 radians	22
9	Curves showing the location of the furthest points that can be reached by trajectories with four switch times for several values of $T(T^2 = 2, 4, 6, 8,$ and $10)$ when the final orientation is 0.8 radians	24
10	Curves showing the location of points that can be reached by trajectories with four switch times for several values of $T(T^2 = 4, 6, 8,$ and $10)$ when the final orientation is 3.14 radians	25
11	Cartesian trajectories for paths with four switch times for a constant value of $T(T^2 = 10)$ when the final orientation is 0.8 radians	25
12	Cartesian trajectories for paths with four switch times for a constant value of $T(T^2 = 10)$ when the final orientation is 3.14 radians	26

Fig.		Page
13	Dual variables for a three-switch-time trajectory leading to the point (0.66, 4.03)	28
14	Dual variables for a four-switch-time trajectory leading to the configuration (0.20, 3.43, 0.80)	29
15	Comparison of four-switch time trajectories of Type 22 and three-switch-time trajectories	30
16	Comparison of four-switch-time trajectories of Type 13 and three-switch-time trajectories	31
17	Comparison of five-switch-time trajectories of Type 23+− and four-switch-time trajectories of Type 22+−	32
18	Comparison of five-switch-time trajectories of Type 23+− and four-switch-time trajectories of Type 13+−	32
19	Comparison of five-switch-time trajectories of Type 23++ and four-switch-time trajectories of Type 13++	33
20	Comparison of five-switch-time trajectories of Type 14+− and four-switch-time trajectories of Type 13	33
21	Comparison of five-switch-time trajectories of Type 14++ and four-switch-time trajectories of Type 13	34

ABSTRACT

This paper addresses the problem of time-optimal motions for a mobile platform in a planar environment. The platform has two non-steerable independently driven wheels. The overall mission of the robot is expressed in terms of a sequence of via points at which the platform must be at rest in a given configuration (position and orientation). The objective is to plan time-optimal trajectories between these configurations assuming an unobstructed environment.

Using Pontryagin's maximum principle (PMP), we formally demonstrate that all time optimal motions of the platform for this problem occur for bang-bang controls on the wheels (at each instant, the acceleration on each wheel is either at its upper or lower limit). The PMP, however, only provides necessary conditions for time optimality. To find the time optimal robot trajectories, we first parameterize the bang-bang trajectories using the switch times on the wheels (the times at which the wheel accelerations change sign). With this parameterization, we can fully search the robot trajectory space and find the switch times that will produce particular paths to a desired final configuration of the platform. We show numerically that robot trajectories with three switch times (two on one wheel, one on the other) can reach any position, while trajectories with four switch times can reach any configuration. By numerical comparison with other trajectories involving similar or greater numbers of switch times, we then identify the sets of time-optimal trajectories. These are uniquely defined using ranges of the parameters, and consist of subsets of trajectories with three switch times for the problem when the final orientation of the robot is not specified, and four switch times when a full final configuration is specified. We conclude with a description of the use of the method for trajectory planning for one of our robots, and discuss some comparisons of sample time-optimal paths with minimum-length paths.

1. INTRODUCTION

A variety of platform designs have been implemented for mobile robots. These can be classified in three major categories: 1. omnidirectional platforms, that utilize steerable wheels [e.g., see robots in Brooks (1990), Arkin (1990), or Koren and Borenstein (1991)], roller-equipped wheels [e.g., see Blaisdell (1991)] or orthogonal wheel assemblies [e.g., see Killough and Pin (1990)]; 2. car-like platforms that incorporate controlled steerable wheels on one axle and non-steerable wheels on another axle [e.g., see Vasseur, Pin, and Taylor (1991)]; and 3. skid-steer platforms that include two non-steerable independently driven wheels [e.g., see Giralt, Chatila, and Vaisset (1984), Kanayama and Hartman (1989), or Weisbin et al. (1989)]. This paper is concerned with skid-steer platforms. A typical mission for a mobile robot can be described by a sequence of via points at which the robot comes to rest in a given configuration (position and orientation) to perform a given task (manipulation, sensing, etc.). The problem considered in this paper is that of finding time-optimal motions of the robot in Cartesian space and the corresponding control trajectories that will move the robot from an initial configuration to a final configuration in an unobstructed environment.

The proposed approach to find the control trajectories that lead to time-optimal motions of the platform involves utilization of Pontryagin's maximum principle [Pontryagin et al. (1986)]. A variety of authors [Kahn and Roth (1971), Niv and Auslander (1984), Kim and Shin (1985), Weinreb and Bryson (1985), Nakamura and Hanafusa (1987), Bobrow (1988), Yamamoto and Mohri (1989)] have applied the maximum principle to the optimal motion planning of serial-link manipulators. For the time optimal motion of a manipulator with bounded control torques, the controls occur linearly in the Hamiltonian and the optimal values of the controls are determined by the dual variables. When its dual variable is not zero, the optimal control is bang-bang (the optimal control is at its upper limit for a positive dual variable and at its lower limit for a negative dual variable). When its dual variable is zero for a finite interval, the optimal control is singular and will be in the region between the bounds. An important issue is to determine when the optimal solution is bang-bang and when it is singular. A variety of authors [Ailon and Langholtz (1985), Wen (1986), Willigenburg (1990), and Chen and Desrochers (1990)] have addressed this issue and proven that there cannot be a finite time interval when the optimal control for a manipulator is singular for all the control torques. In other words, at least one of the controls is always bang-bang. Further work by Geering, et al. (1986) led to the determination of the parameter values for singular solutions for three types of manipulators: cylindrical, spherical, and two link planar. It has been demonstrated [Osipov and Formal'skii (1990), Formal'skii and Osipov (1990)] that the singular solution for the cylindrical case is not optimal. As discussed in the next section, the kinematics of a two-wheeled robot differ significantly from that of a serial-link manipulator and, to our knowledge, the time optimal trajectories for a two-wheeled robot have never been found.

2 *INTRODUCTION*

In the following sections, we present the equations of motion for a skid-steer type of platform moving on a flat, horizontal plane. We then use the maximum principle to derive the conditions for time-optimal motions of the platform and demonstrate that the optimal controls are always bang-bang. Using this result, we show that, for a system with bounded wheel accelerations, control trajectories with three switch times (times at which one of the wheel's acceleration changes sign) allow the robot to reach any point in Cartesian space while with four switch times, the robot can reach any configuration. We then show numerically that these paths are time-optimal.

2. KINEMATIC EQUATIONS OF MOTION FOR THE PLATFORM

A skid-steer type of platform must satisfy nonholonomic constraints and cannot follow an arbitrary path through configuration space. In this section, we develop a kinematic model of the platform, assuming that the wheels do not slip and that the wheel accelerations can instantaneously switch from their upper limit to their lower limit. The configuration of the platform is described by three coordinates: the Cartesian coordinates, x and y, of the midpoint of the wheel axle with respect to an absolute reference frame, and the orientation, ϕ, of the platform main axis with respect to the reference frame x axis (see Fig. 1). The joint variables are the wheels' translational displacements, denoted by θ_R and θ_L, (representing the angular rotation times the radius of the right and left wheels), and are measured in meters. The wheel velocities are denoted by ω_R and ω_L and are measured in meters per second. The control variables are the right and left wheel's translational accelerations (u_R and u_L). The kinematic model links the Cartesian variables to the control variables through the wheel velocities:

$$\dot{\phi} = (\omega_R - \omega_L)/D \tag{1}$$

$$\dot{x} = (\omega_R + \omega_L)\cos(\phi)/2 \tag{2}$$

$$\dot{y} = (\omega_R + \omega_L)\sin(\phi)/2 \tag{3}$$

$$\dot{\omega}_R = u_R \tag{4}$$

$$\dot{\omega}_L = u_L \tag{5}$$

$$\dot{\theta}_R = \omega_R \tag{6}$$

$$\dot{\theta}_L = \omega_L \tag{7}$$

where D is the distance between the centers of the wheels.

Given a trajectory for the control variables, Eqs. (1) through (7) can be integrated to determine the Cartesian variables and the joint variables. Contrary to what is typically the case for serial link manipulators, the time sequence of the controls is necessary to determine the final position of a two-wheeled platform. For example, if both wheels rotate together and move a meter, the platform will move straight forward a meter, while if the right wheel moves a meter first and then the left wheel moves a meter, the platform will move to the left to a point less than a meter away. Although the final values of the joint variables and the final platform orientation are the same for the two maneuvers, the final values for the platform position are not the same.

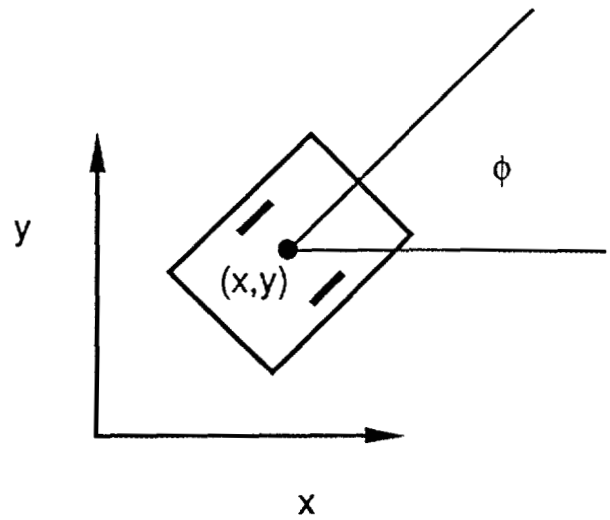

Fig. 1. The configuration of the platform is defined by the position (x,y) and orientation (ϕ).

3. THE GENERAL FORM OF THE OPTIMAL CONTROLS

Since its discovery in 1956, the Pontryagin maximum principle [Pontryagin (1986)] has been used to solve a wide variety of optimization problems. In this section we utilize the maximum principle to derive the conditions for time optimality of the platform motion between the initial and final configurations. For our problem, we can define five state variables: $x_1 = x, x_2 = y, x_3 = \phi, x_4 = \omega_R$, and $x_5 = \omega_L$ and rewrite the equations of motion (1) to (5) as:

$$\dot{x}_1 = f_1(x,u) = (x_4 + x_5)\cos x_3/2 \tag{8}$$

$$\dot{x}_2 = f_2(x,u) = (x_4 + x_5)\sin x_3/2 \tag{9}$$

$$\dot{x}_3 = f_3(x,u) = (x_4 - x_5)/D \tag{10}$$

$$\dot{x}_4 = f_4(x,u) = u_1 \tag{11}$$

$$\dot{x}_5 = f_5(x,u) = u_2 \tag{12}$$

where the two control variables are: $u_1 = u_R$ and $u_2 = u_L$.

In vector notation, the equations of motion for the state vector x are:

$$\dot{x} = f(x,u) \quad , \tag{13}$$

and the optimization problem is to find a control vector $[u]$ that will move the system from the initial state x^0 to the final state x^1 while minimizing an objective functional. For our case, the goal is to minimize the transition time, assuming that the wheel accelerations are bounded: $|u_1| \leq a_{\max}$ and $|u_2| \leq a_{\max}$.

Pontryagin introduces a system of dual variables $[\psi]$ that satisfy:

$$\dot{\psi}_i = -\sum_{j=1}^{n} \frac{\partial f_j(x,u)}{\partial x_i}\psi_j, \quad i = 1,2,\ldots,n \quad , \tag{14}$$

with initial conditions:

$$\psi_i(t_0) = \lambda_i \qquad i = 1,2,\ldots,n \quad , \tag{15}$$

where, in our problem, $n = 5$.

If we choose an admissible control and have the solution of Eq. (13), Eqs. (14) are linear and homogeneous and have a unique solution for given initial conditions. If the equations of motion and the dual variables are combined into a single Hamiltonian H:

$$H(\psi, x, u) = \sum_{j=1}^{n} \psi_j f_j(x, u) \quad , \tag{16}$$

then the PMP states that [see Theorem 2 in Pontryagin (1986)], if u is an admissible control that transfers the phase point from the initial state $x(t_0) = x^0$ to the goal state $x^1 = x(t_1)$ at some time t_1, then $u(t)$ and the trajectory $x(t)$ are time-optimal if there exists a non-zero continous vector function $(\psi_1(t), \ldots \psi_n(t))$ defined by Eq. (14), and such that $u(t)$ maximizes the function H for all t, $t_0 \leq t \leq t_1$.

For our mobile platform problem defined by Eqs. (8) through (12), the Hamiltonian function H is:

$$H(\psi, x, u) = \psi_1 f_1 + \psi_2 f_2 + \psi_3 f_3 + \psi_4 u_1 + \psi_5 u_2 \tag{17}$$

where the functions $f_i(x, u)$ are defined by Eqs. (8) to (12). The equations for the dual variables are:

$$\dot{\psi}_1 = 0 \tag{18}$$

$$\dot{\psi}_2 = 0 \tag{19}$$

$$\dot{\psi}_3 = g(x_3)(x_4 + x_5) \tag{20}$$

$$\dot{\psi}_4 = -g'(x_3) - \psi_3/D \tag{21}$$

$$\dot{\psi}_5 = -g'(x_3) + \psi_3/D \tag{22}$$

where $g(x_3)$ and $g'(x_3)$ are defined by:

$$g(x_3) = (\psi_1 \sin x_3 - \psi_2 \cos x_3)/2 \tag{23}$$

$$g'(x_3) = \frac{dg(x_3)}{dx_3} = (\psi_1 \cos x_3 + \psi_2 \sin x_3)/2 \tag{24}$$

The platform moves from an arbitrary initial configuration to an arbitrary final configuration. We can choose the coordinate system such that the initial position is (0,0) and the initial orientation is $\phi = 0$. The boundary conditions corresponding to the robot being at rest at the initial state $x^0 = x(t_0)$ and final state $x^1 = x(t_1)$, are

$$x(t_0) = (0, 0, 0, 0, 0) \tag{25}$$

$$x(t_1) = (x, y, \phi, 0, 0) \tag{26}$$

When the final state is fully specified (position and orientation are given), the final values of the dual variables are arbitrary. When the final state is not fully specified, the transversality condition determines the final values of the dual variables [see Theorem 3 in Pontryagin (1986)]. For example, when the final state is a position (and the final orientation is not specified), the final value of the third dual variable (ψ_3) must be zero.

The optimal values for the control variables (u_1 and u_2) are those that maximize the Hamiltonian. From Eq. (17), it is clear that when the dual variables ψ_4 and ψ_5 are not zero, the optimal control is bang-bang; when ψ_4 is positive, $u_1 = a_{\max}$ and when ψ_4 is negative, $u_1 = -a_{\max}$, and similarly for ψ_5 and u_2. If ψ_4 or ψ_5 is zero for a finite time interval, the optimal control becomes singular. In the remaining of this section we will prove that all possible optimal solutions of the system are bang-bang.

Theorem

All optimal control solutions for the system defined by Eqs. (8) through (12), (25) and (26) are bang-bang.

Proof

From Eq. (17), we know that when the dual variables ψ_4 and ψ_5 are not zero, the optimal control is bang-bang; and when ψ_4 or ψ_5 is zero for a finite interval, the optimal control is singular. To prove the theorem, we will investigate all the singular solutions and show that they are either impossible or bang-bang.

When the optimal control is singular, ψ_4 (or ψ_5) is zero for a finite interval. If ψ_4 is zero for a finite time interval, $[t_2, t_3]$, all of its derivatives are also zero on the interval and Eq. (21) yields:

$$\psi_3 = -Dg'(x_3) \tag{27}$$

The time derivative of Eq. (27) implies:

$$\dot{\psi}_3 = -D\frac{dg'(x_3)}{dx_3}\dot{x}_3 = g(x_3)(x_4 - x_5) \tag{28}$$

where we have used the fact that $\frac{dg'(x_3)}{dx_3} = -g$.

Since the right sides of Eqs. (20) and (28) must be equal, we have:

$$g(x_3)x_5 = 0 \tag{29}$$

Both $g(x_3)$ and x_5 are continuous functions. If there is a point in $[t_2, t_3]$ where x_5 is not equal to zero, then there is a finite interval where x_5 is not equal to zero and on this subinterval $g(x_3)$ is zero. Similarly, if there is a point in $[t_2, t_3]$ where $g(x_3)$

is not equal to zero, then there is a subinterval where x_5 is zero. Thus, we will consider two general cases:

$$\text{Case 1.} \quad g(x_3) = 0 \tag{30}$$

$$\text{Case 2.} \quad x_5 = 0 \tag{31}$$

To simplify the notation, we will continue to label the subintervals of $[t_2, t_3]$ where Eqs. (30) or (31) are valid $[t_2, t_3]$.

Case 1 can be subdivided into four subcases:

$$\text{Case 1.1.} \quad \psi_1 \neq 0 \quad , \quad \psi_2 \neq 0. \tag{32}$$

$$\text{Case 1.2.} \quad \psi_1 = 0 \quad \psi_2 \neq 0. \tag{33}$$

$$\text{Case 1.3.} \quad \psi_1 \neq 0 \quad \psi_2 = 0. \tag{34}$$

$$\text{Case 1.4.} \quad \psi_1 = \psi_2 = 0 \tag{35}$$

For the first three subcases, x_3 is a constant on the interval $[t_2, t_3]$:

Case 1.1. $\tan x_3 = \psi_2/\psi_1$

Case 1.2. $\cos x_3 = 0$

Case 1.3. $\sin x_3 = 0$

Consider Cases 1.1, 1.2, and 1.3

Since ψ_1 and ψ_2 are constant (from Eqs. (18) and (19)) and $g(x_3) = 0$, x_3 is a constant and $\dot{x}_3 = 0$ on the finite interval $[t_2, t_3]$. Thus, these cases correspond to the robot moving along a straight line over a finite interval of time, (the angle $\phi = x_3$ given by Eqs. (32), (33), or (34)) and Eq. (10) requires that $x_4 = x_5$, i.e., that the controls on both wheels be equal, $u_1 = \dot{x}_4 = \dot{x}_5 = u_2$, over the interval $[t_2, t_3]$. Now, since $g = 0$, $\dot{\psi}_3 = 0$ (using Eq. (20)), and ψ_3 is a constant. Since g' is also a constant (ψ_1, ψ_2, and x_3 are constants in Eq. (24)), $\dot{\psi}_5$ is constant (from Eq. (22)).

If $\dot{\psi}_5$ is a non-zero constant, then ψ_5 varies linearly, and the optimal controls u_2 and u_1 are equal and bang-bang over the interval $[t_2, t_3]$. If $\dot{\psi}_5$ is zero, then Eq. (22) yields $\psi_3 = Dg'(x_3)$ which, with Eq. (27), implies $\psi_3 = g'(x_3) = 0$. If both $g = 0$ and $g' = 0$, then $\psi_1 = \psi_2 = 0$. This violates the assumptions in Eqs. (32), (33), or

(34) and consequently $\dot{\psi}_5 = 0$ is not a valid solution for these cases. Thus, for cases 1.1, 1.2, and 1.3, the only admissible controls are bang-bang.

Consider Case 1.4

If $\psi_1 = \psi_2 = 0$ over the interval $[t_2, t_3]$, they are also zero over the entire trajectory (from Eqs. (18) and (19)). Thus $g = g' = 0$ and $\dot{\psi}_3 = 0$ (from Eq. (20)) over the entire trajectory. Furthermore, since ψ_3 is a constant and $\psi_3 = 0$ (from Eq. (27)) on the interval $[t_2, t_3]$, $\psi_3 = 0$ over the entire trajectory. Consequently, $\dot{\psi}_5 = 0$ from Eq. (22), requiring the dual variable ψ_5 to be constant over the entire trajectory. This is not an admissible case for our problem since the corresponding extremal controls u_2 would not change sign over the entire trajectory, leading to a linearly increasing or decreasing wheel velocity and making Eq. (26) impossible to satisfy. Thus case 1.4 does not lead to admissible controls for our problem.

Consider Case 2

If $x_5 = 0$ over a finite time interval $[t_2, t_3]$, then the control $u_2 = \dot{x}_5 = 0$ over the interval, and consequently its dual variable ψ_5 and its derivative $\dot{\psi}_5$ must be zero over the entire finite interval. Since $\psi_4 = \dot{\psi}_4 = 0$, Eqs. (21) and (22) require $\psi_3 = 0$ and $g'(x_3) = 0$ over the entire interval, and consequently $\dot{\psi}_3 = 0$. Equation (20) thus requires either that $x_4 = x_5 = 0$, which is an inadmissible case (since, from Eqs. (8) through (12), no motion of the robot would take place over a finite time interval during the trajectory, which consequently can not be time optimal), or that $g(x_3) = 0$ over the finite time interval. If both g and g' are zero over the finite time interval, then $\psi_1 = \psi_2 = 0$. Since ψ_1 and ψ_2 are constant over the entire trajectory (from Eqs. (18) and (19)), they must be zero over the entire trajectory and Eq. (23), (24), and (20) lead to $g = g' = \dot{\psi}_3 = 0$ over the entire trajectory. Consequently, since $\psi_3 = 0$ over the finite time interval and $\dot{\psi}_3 = 0$ over the entire trajectory, $\psi_3 = 0$ and $\dot{\psi}_4 = \dot{\psi}_5 = 0$ (from Eqs. (21) and (22)) over the entire trajectory. Therefore, since $\psi_4 = 0$ and $\psi_5 = 0$ over the finite interval, they also are zero on the entire trajectory. Thus this case is not admissible since all dual variables ψ_i are zero over the entire trajectory.

Since the equations for ψ_4 and ψ_5 have the same structure, similar arguments demonstrate that singular solutions corresponding to the dual variable ψ_5 being zero over a finite time interval lead to optimal controls that are bang-bang, or are inadmissible.

If $\psi_4 = \psi_5 = 0$ over a finite interval $[t_2, t_3]$, then $\dot{\psi}_4 = \dot{\psi}_5 = 0$ over the interval and Eqs. (21) and (22) require that $g'(x_3) = \psi_3 = 0$ over the interval. Since ψ_1 and ψ_2 are constant, $g'(x_3) = 0$ implies that x_3 is constant over the entire interval. Thus $\dot{x}_3 = 0$ and, from Eq. (10), $x_4 = x_5$ over the entire interval. On the other hand, $\psi_3 = 0$ over the entire interval implies $\dot{\psi}_3 = 0$, and Eq. (20) requires either $x_4 = -x_5$ which, with the conclusion of the previous sentence, leads to $x_4 = x_5 = 0$

(i.e., the robot does not move during the entire interval), which is not an admissible solution; or $g(x_3) = 0$, which has been treated as Case 1 above and shown to lead to bang-bang or inadmissible controls. Thus, all optimal control solutions for the system defined by Eqs. (8) through (12), (25), and (26) are bang-bang.

A similar result was recently outlined by Jacobs, Laumond and Rege (1991), however, without consideration given to cases 1.2, 1.3, 1.4, and $\psi_4 = \psi_5 = 0$ in the demonstration.

4. PARAMETERIZATION OF THE BANG-BANG TRAJECTORIES

The Pontryagin maximum principle converts the problem of time-optimal path planning from a problem involving trajectories in state space and time to a static optimization problem in parameter space. Two sets of parameters are available: the initial conditions for the dual variables $[\lambda_k]$ and the switch times. Using either set of parameters, nonlinear search techniques can be used to determine bang-bang control trajectories that move the robot from the initial state to the final state. In the remainder of this paper, we will use the switch times to parameterize the control trajectories and the corresponding robots paths. The PMP provides necessary (but not sufficient) conditions for an optimal trajectory. In the following sections, we will indeed find trajectories that satisfy the necessary conditions but are not time-optimal. To show that a bang-bang trajectory is time-optimal, we must show that it satisfies the necessary conditions and that the corresponding robot path is faster than all alternative paths.

To show that a bang-bang trajectory satisfies the necessary conditions, we will numerically integrate the controls of the wheels to calculate the Cartesian path of the robot and some auxiliary variables, use the auxiliary variables to calculate the initial conditions for the dual variables, numerically integrate to calculate the dual variables, and verify that the necessary conditions are satisfied by showing that the dual variables are consistent with the bang-bang controls. In this section, we parameterize the trajectories, define the auxiliary variables, and show how to calculate the initial conditions for the dual variables. In the next two sections, we will explore the space of bang-bang trajectories and uniquely identify those that are time-optimal.

We have proven that the optimal controls are bang-bang. Thus, each wheel is always either accelerating or decelerating at the maximum rate ($a_{\max}$), and the wheel velocity trajectories consist of successive segments of linearly increasing or decreasing velocity. The wheel acceleration changes sign at a switch time. We can characterize a wheel control trajectory by its number of switch times, and a robot path by its total number of switch times and their distribution on either of the two wheels. We will find that, for given total trajectory times, a specific set of robot paths with a small number of switch times reach farther (and therefore are faster) than all paths with a larger number of switch times. At the lower bound, the path with the smallest number of switch times has two (one for each wheel). However, there are only two paths with two switch times: a translation straight forward and a pure rotation. On the other hand, we know that the minimum length paths for a skid-steer platform consist of sequences of translations and rotations. A rotation followed by a translation can reach any position and requires five switch times, while a path consisting of a rotation, a translation, and a rotation can reach any configuration and has eight switch times. In the next section, we will show that the robot can reach any position in the plane using specific paths involving a total of three switch times (one on one wheel, two on the other), and does so faster than

with a greater number of switch times. Similarly, we will show that, using specific paths with four switch times, the robot can reach any configuration faster than with paths involving a greater number of switch times.

First, we derive an analytical expression for the displacement of a single wheel with four switch times. By adjusting parameters, the expression will yield the displacement for motions with one, two, or three switch times. We assume that the initial value for the wheel displacement (θ) is zero. Since the initial and final values for the wheel velocity are zero, the wheel will accelerate during half of the trajectory time, and it will decelerate during the other half. We will denote by T half of the total trajectory time.

A control trajectory with four switch times has five time segments denoted by (τ_i). For two wheels, we can define ten segments; our notation for the right segments will be (τ_1, τ_3, τ_5, τ_7, τ_9), while the left segments will be (τ_2, τ_4, τ_6, τ_8, τ_{10}). Let u_R be the initial acceleration on the right wheel. The control trajectory for the right wheel will be: u_R for $[0, \tau_1]$, $-u_R$ for $[\tau_1, \tau_1 + \tau_3]$, u_R for $[\tau_1 + \tau_3, \tau_1 + \tau_3 + \tau_5]$, $-u_R$ for $[\tau_1 + \tau_3 + \tau_5, \tau_1 + \tau_3 + \tau_5 + \tau_7]$, and u_R for $[\tau_1 + \tau_3 + \tau_5 + \tau_7, 2T]$. Since the wheel will accelerate during half of the trajectory, and it will decelerate during the other half:

$$\tau_1 + \tau_5 + \tau_9 = \mathrm{T} \tag{36}$$

$$\tau_3 + \tau_7 = \mathrm{T} \tag{37}$$

Integrating Eqs. (4) and (6), we can calculate the final value of the right wheel displacement for a four-switch-time trajectory of that wheel:

$$\theta_R(2\mathrm{T}) = u_R[-2\tau_3\tau_5 + 2(\tau_1 + \tau_5)\mathrm{T} - \mathrm{T}^2] \tag{38}$$

Equation (38) relates the wheel displacement to the first three segments. Using Eqs. (36) and (37), we can relate the wheel displacement to the last three segments:

$$\theta_R(2\mathrm{T}) = u_R[2\tau_5\tau_7 - 2(\tau_5 + \tau_9)\mathrm{T} + \mathrm{T}^2] \tag{39}$$

The similar expressions for the displacement of the left wheel are:

$$\tau_2 + \tau_6 + \tau_{10} = \mathrm{T} \tag{40}$$

$$\tau_4 + \tau_8 = \mathrm{T} \tag{41}$$

$$\theta_L(2\mathrm{T}) = u_L[-2\tau_4\tau_6 + 2(\tau_2 + \tau_6)\mathrm{T} - \mathrm{T}^2] \tag{42}$$

$$\theta_L(2\mathrm{T}) = u_L[2\tau_6\tau_8 - 2(\tau_6 + \tau_{10})\mathrm{T} + \mathrm{T}^2] \tag{43}$$

with u_L representing the initial acceleration of the left wheel.

4.1 ANALYTICAL RELATIONSHIP BETWEEN THE SEGMENTS AND THE FINAL ORIENTATION

Although the equations of motion for the Cartesian position variables (x, y) do not have general analytical solutions, a solution for the Cartesian orientation variable ϕ can be derived analytically. Using Eqs. (6) and (7), Eq. (1) may be written:

$$\dot{\phi} = (\dot{\theta}_R - \dot{\theta}_L)/D \tag{44}$$

Since the initial conditions for the wheel displacement joint variables are zero, Eq. (44) can be integrated to yield:

$$\phi = \phi_0 + (\theta_R - \theta_L)/D \tag{45}$$

where ϕ_0 is the initial value of the robot's orientation.

Equations (38), (39), (42), and (43) relate the segment lengths to the wheels' displacement, while Eq. (45) relates the wheels' displacement to the change in orientation. Given segment lengths for both wheels, the final change in orientation can be calculated. Alternatively, given the desired final orientation of the robot, Eq. (45) provides a constraint on the segment lengths.

Consider a robot path involving three switch times; one on the right wheel and two on the left wheel (the segment lengths are: $\tau_1 = \tau_3 = \tau_4 = \mathrm{T}$, and $\tau_5 = \tau_7 = \tau_8 = \tau_9 = \tau_{10} = 0$). Since $\tau_2 + \tau_6 = T$, this path is defined by two parameters (τ_2 and T). Using Eqs. (39) and (43), the final wheel displacements are:

$$\theta_R = u_R \mathrm{T}^2 \tag{46}$$

$$\theta_L = u_L[T^2 - 2\tau_6 \mathrm{T}] \tag{47}$$

Since the initial value of the robot's orientation is zero, the final change in orientation is:

$$\phi D = u_R \mathrm{T}^2 - u_L[\mathrm{T}^2 - 2\tau_6 \mathrm{T}] \tag{48}$$

If $u_R = u_L = u$, the final orientation is:

$$\phi D = 2u\tau_6 \mathrm{T} \tag{49}$$

while if $u_R = -u_L = u$, the final orientation is:

$$\phi D = 2u\tau_2 \mathrm{T} \tag{50}$$

If the final orientation is specified and is positive (negative), then u must be positive (negative). Moreover, if a final orientation is specified for a three-switch-times path, Eqs. (49) and (50) may not have acceptable solutions for small values of T, since $0 \leq \tau_i \leq \mathrm{T}$. On the other hand, if no constraint on the final orientation is specified for a path, Eqs. (49) and (50) show that as τ_2 or τ_6 varies from zero to T, the

change in orientation varies continuously from zero (the motion is a translation straight forward) to $2u\mathrm{T}^2/D$ (the motion is a pure rotation).

4.2 CALCULATION OF THE DUAL VARIABLES

To verify that a bang-bang trajectory satisfies the necessary conditions, we must calculate the dual variables and show that they are consistent with the control paths [i.e., that u_1 is positive (negative) when ψ_4 is positive (negative), etc.]. The dual variables satisfy Eqs. (18) to (22), with initial conditions given by Eq. (15). Since this set of equations is linear and homogeneous, it has a unique solution for any set of initial conditions (λ_i). Thus, the initial conditions determine the trajectories of the dual variables. From Eqs. (18) and (19), the first two dual variables are constants ($\psi_1 = \lambda_1$ and $\psi_2 = \lambda_2$). Using Eqs. (8), (9), (20), and (23), the third dual variable satisfies:

$$\dot{\psi}_3 = \psi_1 \dot{x}_2 - \psi_2 \dot{x}_1 \tag{51}$$

Since the initial position is (0,0), Eq. (51) can be integrated:

$$\psi_3 = \lambda_1 x_2 - \lambda_2 x_1 + \lambda_3 \tag{52}$$

The fourth and fifth dual variables satisfy Eqs. (21) and (22). The right sides of these equations depend on the first three state variables. To integrate the equations, we define four auxiliary variables (z_i) by:

$$\dot{z}_1 = \sin(x_3) \qquad z_1(0) = 0 \tag{53}$$

$$\dot{z}_2 = \cos(x_3) \qquad z_2(0) = 0 \tag{54}$$

$$\dot{z}_3 = x_1 \qquad z_3(0) = 0 \tag{55}$$

$$\dot{z}_4 = x_2 \qquad z_4(0) = 0 \tag{56}$$

Using the auxiliary variables, the solutions for the fourth and fifth dual variables are:

$$\psi_4 = -\lambda_1(z_2/2 + z_4/D) + \lambda_2(z_3/D - z_1/2) - \lambda_3(\tau/D) + \lambda_4 \tag{57}$$

$$\psi_5 = \lambda_1(z_4/D - z_2/2) - \lambda_2(z_1/2 + z_3/D) + \lambda_3(\tau/D) + \lambda_5 \tag{58}$$

Since the switch times of a trajectory correspond to times when either ψ_4 or ψ_5 changes sign, one of the dual variables must be zero at the switch time. Thus, the initial conditions for the dual variables can be determined by solving the matrix equation: $A\lambda = 0$, where $\lambda^{\mathrm{T}} = (\lambda_1, \ldots, \lambda_5)$ and the rows of the matrix A are defined by either Eqs. (57) or (58) applied at the switch times. If the switch time

is for the right wheel, ψ_4 is equal to zero and Eq. (57) defines a row of A. If the switch time is for the left wheel, ψ_5 is equal to zero and Eq. (58) defines a row of A. It is interesting to note here that, in the general case, a control path with n switch times will produce a matrix with n rows. For the vector λ to be nonzero, the rank of A must be four or less. In other words, if a control path has less than five switch times, a nonzero solution is possible. If the control path has more than four switch times, the columns of the A matrix must be linearly dependent. Thus, in the next section, we will first explore the space of robot paths involving four switch times in order to investigate general solutions of our problem when the final configuration (position and orientation) is specified. A particular case occurs when the final state is a position (and the final orientation is not specified). In that case, the transversality condition [see Pontryagin (1986) Theorem 3, page 50] requires that the final value of the third dual variable be zero and Eq. (52) defines a row of A. Thus, when the final state is a position, a path with three switch times would produce a four row matrix. In the next section, we will therefore explore the space of robot paths involving three switch times to investigate general solutions of the problem when the final orientation is not specified.

5. BANG-BANG TRAJECTORIES

Our objective is to move from an arbitrary initial configuration to an arbitrary final configuration in minimum time. Each configuration is described by three coordinates (x, y, ϕ), where (x, y) is the location of the midpoint between the two wheels and ϕ is the orientation of the robot. We can choose the coordinate system such that the initial configuration is (0,0,0). The initial and final values for the wheel velocities (ω_R and ω_L) are zero.

We will first explore the spaces of paths with three and four switch times. With the parameterization described in the previous section, we can vary the available parameters over the entire range, and for each set of parameter values, we can numerically integrate the equations of motion using a fourth-order Runge-Kutta method [Press (1988)] to determine the Cartesian path of the platform and its final position and orientation. To produce the example figures in this section, we have used $a_{\max} = 0.5$ meters/second^2 for the acceleration bound on the wheels, and $D = 0.76$ meters for the wheels' spacing.

5.1 TRAJECTORIES TO A POINT

When the goal is to reach a given point with no specified orientation, the problem is symmetrical and can be solved considering only the first quadrant. If any point in the first quadrant can be reached, symmetrical points in the other three quadrants can be reached by changing the sign of the wheels' controls, i.e., changing the initial direction of motion (symmetry about the y axis) or by exchanging the trajectories for the two wheels (symmetry about the x axis). Given the symmetry conditions, we are exploring three switch times trajectories involving one switch time for the right wheel and two for the left wheel. As mentioned previously, the three switch time trajectories with no specified final orientation can be parameterized using two parameters and can be of two types, which we refer to as: Type ++ (on the initial segment, $u_R = u_L = u$) and Type +− ($u_R = -u_L = u$).

Figure 2 shows the final locations of the platform for the two types of solutions when one of the parameters, the half timeT of the trajectory, is kept at a fixed value, T = $\sqrt{10}$ sec. The Type ++ trajectories initiate with a translation and end with a rotation, while the Type +− trajectories initiate with a rotation and end with a translation. As the parameter ($\tau = \tau_2$ or τ_6) increases from zero to T, the final positions of the robot for both types of trajectories describe a curve from the point (5,0) to the origin, with the motion varying from a pure translation reaching the point (5,0) for $\tau = 0$, to a pure rotation of the robot at the origin for $\tau =$ T.

Considering the first quadrant and all symmetries involved in the problem, it is clear that the trajectories of Type +− that end on the arc AB, which we thereafter call "first arc," can reach points further away from the origin than the other trajectories of Type +− and all trajectories of the Type ++. In Fig. 3, the final platform locations which correspond to first arcs are plotted for several values of T. Since for pure translation, the platform moves a distance x along the x-axis:

$$x = u\mathrm{T}^2 \quad , \tag{59}$$

we have used the values $\mathrm{T}^2 = 2, 4, 6, 8$, and 10 (consequently, $x = 1, 2, 3, 4$, and 5 when $y = 0$ and $u = a_{\max} = .5$ m/sec). From Figs. 2 and 3 it is clear that, for a constant value of T, the final location of the platform sweeps through the first quadrant on a first arc as the parameter τ increases from zero and, for increasing values of T, the first arcs continuously expand toward higher values of (x, y). Thus, each point in the first quadrant can be reached by a three-switch-time trajectory ending on a first arc, and there is a one-to-one relationship between the points in the first quadrant and the parameter set (T, τ) which uniquely defines the trajectories reaching the first arcs.

Each first arc is uniquely defined by its value of T and the range of the parameter τ required to sweep the first quadrant: $0 \leq \tau \leq \tau^m$, where the value $\tau^m(\mathrm{T})$ corresponds to the intersection with the y axis. The ratio of τ^m and T is displayed in Fig. 4 as a function of T. As discussed previously with Eqs. (49) and (50), there is a minimum half time $\mathrm{T}_{\min}$ required to rotate 90 degrees. For the robot parameter values used in the figures, $\mathrm{T}_{\min} = 1.095$. When T is less than 1.095, τ^m is not defined. When T is equal to 1.095, $\tau^m = \mathrm{T}$ and the ratio is 1.0. As T increases, the ratio decreases as expected, reaching 0.35 when T = 2.0 and 0.09 when T = 4.0.

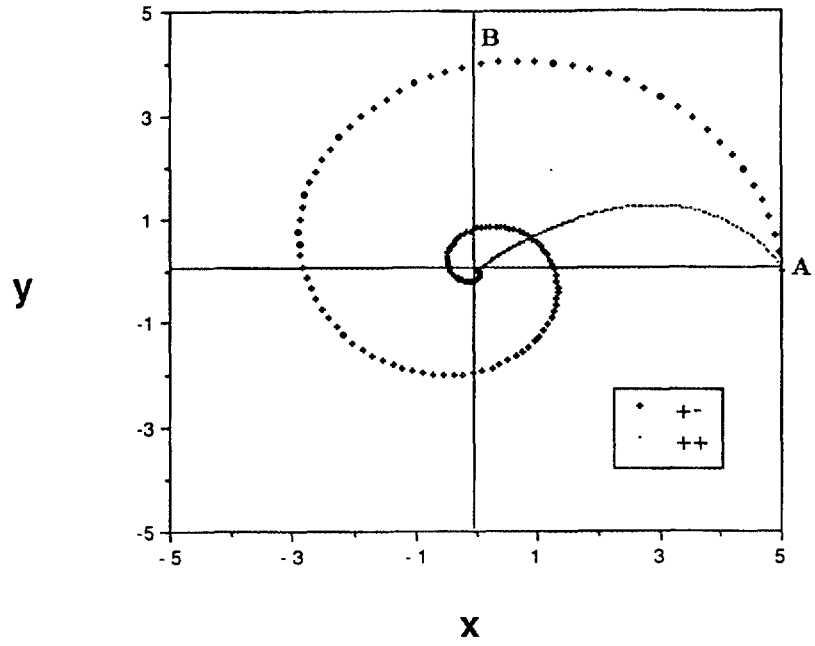

Fig. 2. Points that can be reached by trajectories with three switch times for a constant value of T = $\sqrt{10}$ sec.

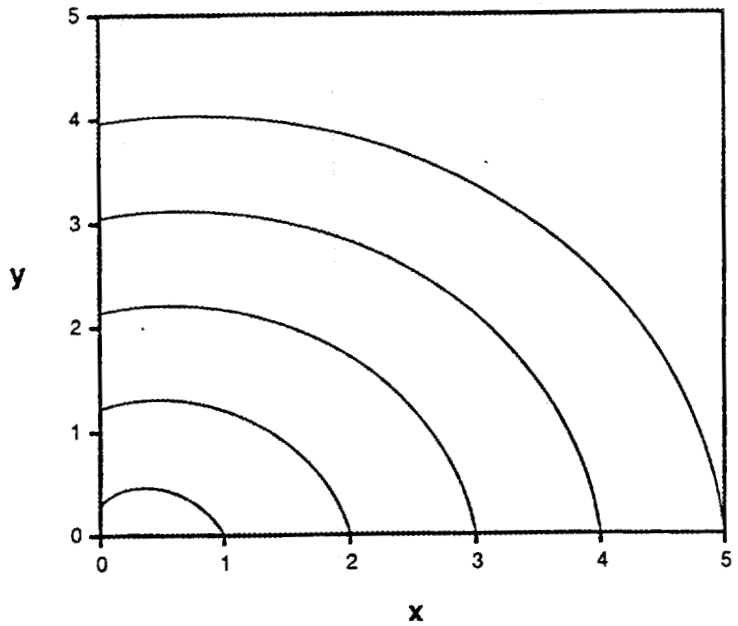

Fig. 3. Curves showing the location of the furthest points in the first quadrant that can be reached by trajectories with three switch times for several values of T ($T^2 = 2, 4, 6, 8$, and 10).

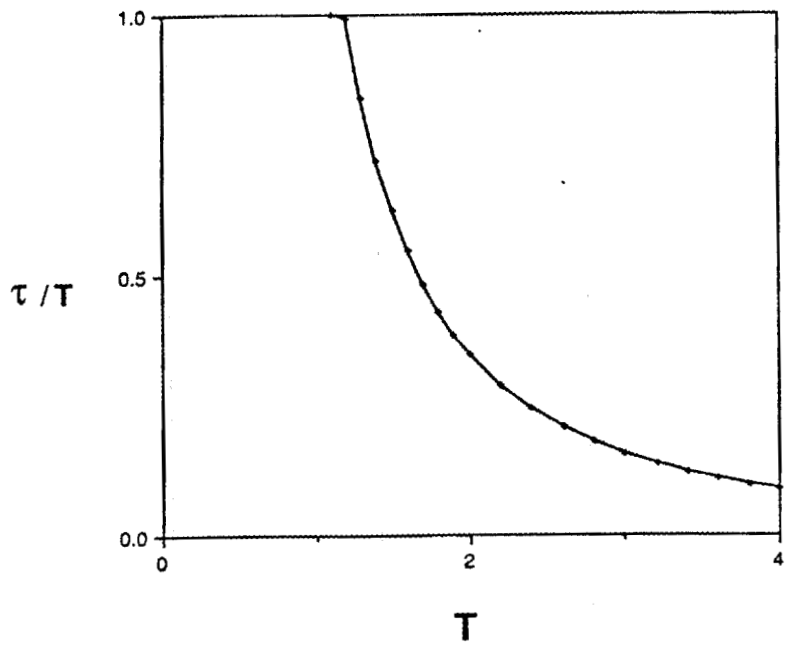

Fig. 4. Curve showing the ratio of τ^m and T. The sets (τ^m, T) define the intersection of the first arcs with the y axis.

Based on the above considerations, the remaining set of three-switch-time trajectories that are candidates for time-optimal trajectories to a point, is the uniquely defined set of trajectories reaching points on first arcs. Sample Cartesian paths of the robot for the candidate three-switch-time trajectories are displayed in Fig. 5 for the case where $T^2 = 10$. Note that, at the end of all paths, both wheels have the same velocity and the Cartesian paths are line segments.

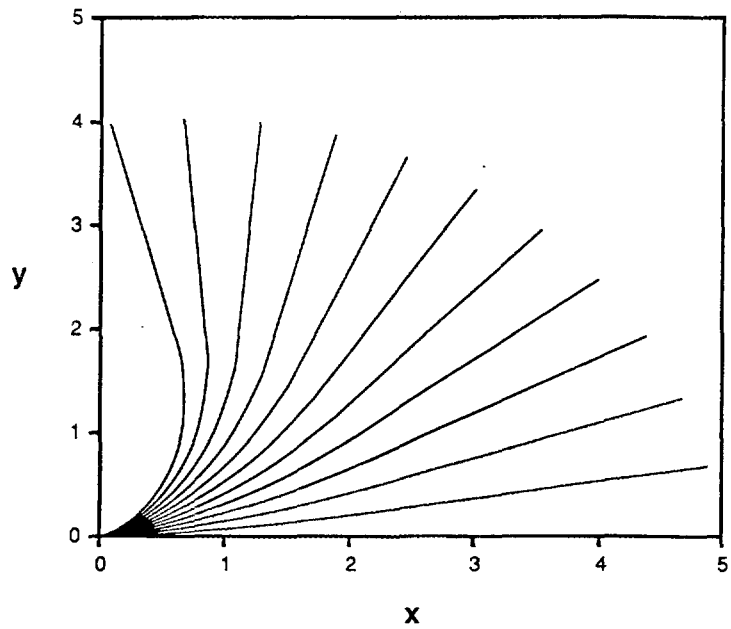

Fig. 5. Cartesian paths of the robot for three-switch-time trajectories ending on the first arc defined by $T^2 = 10$.

5.2 TRAJECTORIES TO A CONFIGURATION

In a similar manner, and based on the discussion of Section 4.2, we can use the parameterization developed in 4.1 to explore the space of four-switch-time trajectories when the goal is to reach a given configuration. In this case, the problem is not symmetrical about the x and y axes and the four quadrants have to be explored.

A four-switch-time trajectory can have either two switch times for each wheel (Type 22) or one switch time for one wheel and three switch times for the other wheel (Type 13). For the Type 22 trajectories, the segment lengths satisfy: $\tau_3 = \tau_4 = T$, $\tau_7 = \tau_8 = \tau_9 = \tau_{10} = 0$, $\tau_1 + \tau_5 = T$ and $\tau_2 + \tau_6 = T$. With these conditions and the constraint on the final orientation given by Eqs. (38), (42), and (45), these trajectories can be defined with two parameters, e.g., τ_1 or τ_2, and T. Similarly, for the Type 13 trajectories, the segment lengths satisfy: $\tau_1 = \tau_3 = T$, $\tau_5 = \tau_7 = \tau_9 = \tau_{10} = 0$, $\tau_2 + \tau_6 = T$, and $\tau_4 + \tau_8 = T$ (one switch time on the right wheel

and three on the left), or: $\tau_2 = \tau_4 = \mathrm{T}$, $\tau_6 = \tau_8 = \tau_9 = \tau_{10} = 0$, $\tau_1 + \tau_5 = \mathrm{T}$, and $\tau_3 + \tau_7 = \mathrm{T}$ (three switch times on the right wheel and one on the left). With the constraint on the final orientation, these trajectories can also be defined with two parameters τ_2 or τ_4, and T; or τ_1 or τ_3, and T.

Figure 6 displays the points that can be reached by four-switch-time trajectories when the orientation is $\phi = 0.8$ radians and $\mathrm{T}^2 = 10$. Since we have two types of trajectories and four combinations of initial acceleration ($++$, $--$, $+-$, $-+$), there are eight curve segments displayed in Fig. 6. There are four significant intersection points (C, D, E, F) in the figure. These are points where the four-switch-time trajectories become three-switch-time trajectories of the Type 12, i.e., where one of their segment τ_i vanishes. For example, the two points, C and D, in the first quadrant are where the two curves in Fig. 2 reach an orientation of 0.8 radians (at the points, Eqs. (49) and (50) are satisfied). All of the eight curve segments start at one of these four points and end at another. The same pattern is observed in Figs. 7 and 8 which display the points that can be reached by four-switch-time trajectories when the final orientation is $\phi = 1.57$ radians and $\phi = 3.14$ radians (and $\mathrm{T}^2 = 10$).

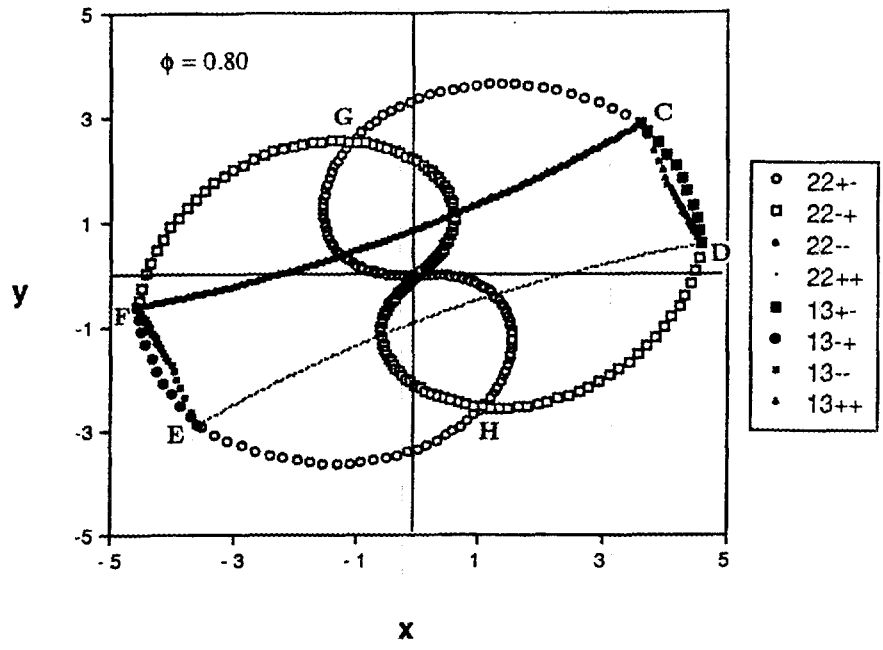

Fig. 6. Points that can be reached by trajectories with four switch times for a constant value of $\mathrm{T}(\mathrm{T}^2 = 10)$ when the final orientation is 0.8 radians.

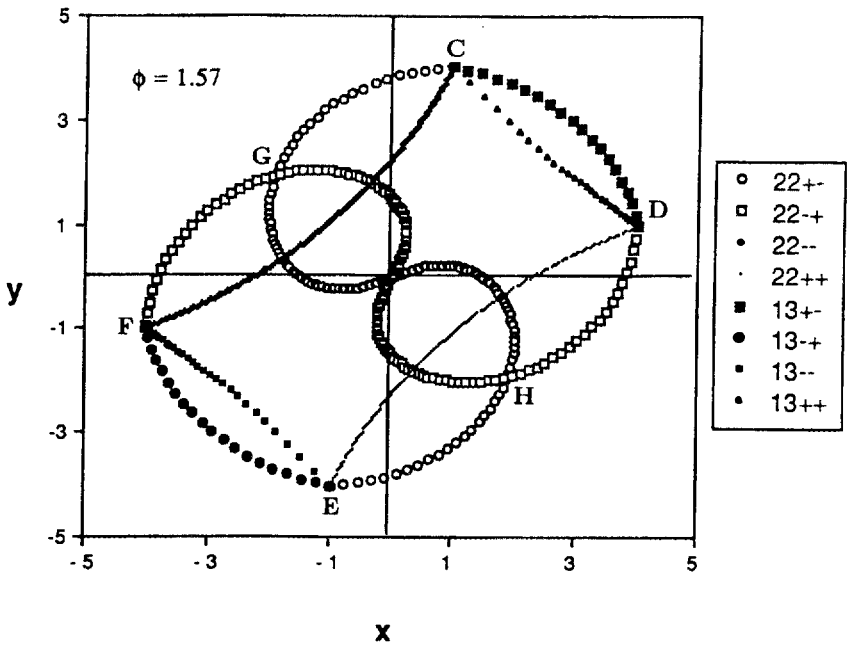

Fig. 7. Points that can be reached by trajectories with four switch times for a constant value of $T(T^2 = 10)$ when the final orientation is 1.57 radians.

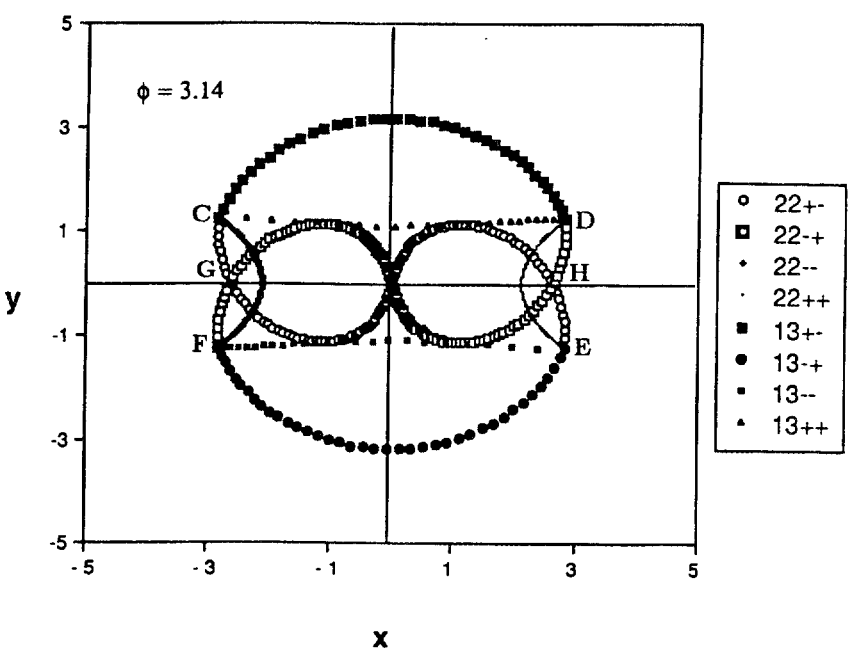

Fig. 8. Points that can be reached by trajectories with four switch times for a constant value of $T(T^2 = 10)$ when the final orientation is 3.14 radians.

Figures 6 and 7 are not symmetrical about the x or y axis. However, we can show that the two axes of symmetry are rotated by $\phi/2$ (thus, Fig. 8 is symmetrical about the x and y axis) and identify the location of the points G and H. Consider an arbitrary bang-bang trajectory that starts at (0,0,0) and reaches (x^1, y^1, ϕ). Suppose that a second trajectory leaves (0,0,0) with the time reverse control trajectory (the length of the initial segment of the second trajectory will be equal to the length of the final segment of the first trajectory but the signs of the control variables will be reversed). The holonomic variables (wheel rotation and final orientation) will be the same for the two trajectories but the nonholonomic variables (x, y) will be different. Thus, the second trajectory will reach (x^2, y^2, ϕ).

If we let time run backwards, the second trajectory is identical to the first and we can derive a mapping from (x^1, y^1) to (x^2, y^2):

$$x^2 = x^1 \cos\phi + y^1 \sin\phi \tag{60}$$

$$y^2 = x^1 \sin\phi - y^1 \cos\phi \tag{61}$$

The mapping applies to any arbitrary bang-bang trajectory. On the first line of symmetry, the second point is the same as the first $[(x^1, y^1) = (x^2, y^2) = (x, y)]$:

$$y/x = \sin\phi/(1 + \cos\phi) = (1 - \cos\phi)/\sin\phi = \tan(\phi/2) \tag{62}$$

Thus, the direction of the first line of symmetry is $\phi/2$. On the second line of symmetry, the second point is reflected through the origin $[(x^1, y^1) = (-x^2, -y^2) = (x, y)]$:

$$y/x = -(1 + \cos\phi)/\sin\phi = -\sin\phi/(1 - \cos\phi) = \tan[(\pi + \phi)/2] \tag{63}$$

Thus, the direction of the second line of symmetry is $(\pi + \phi)/2$.

We can move the final configuration across the first line of symmetry by time reversing the control trajectory. We can move the final configuration across the second line of symmetry by reversing the control trajectory between the wheels and by changing the signs of the controls (if we do not reverse the signs of the wheel rotations, the sign of the final orientation will be reversed).

Just as in Section 5.1, we can define a set of candidates for time-optimality as the set of trajectories reaching furthest in the plane for a given value of T. From Figs. 6 to 8, it can be seen that the envelop ($C\ D\ H\ E\ F\ G\ C$) is reached by trajectories of Type 13+−, 13−+, and some of the Type 22+− and 22−+ that are uniquely defined by the points G and H.

Just like in Section 5.1, we can also show that the candidate four-switch-time trajectories can reach any configuration by varying the half time parameter T. Figures 9 and 10 illustrate the continuous sweeping through all of the points in the plane as the parameter T increases. In Fig. 9 the final orientation is $\phi = 0.80$ radians, while in Fig. 10 the final orientation is $\phi = 3.14$ radians. In both figures, the curves are for $T^2 = 2, 4, 6, 8$, and 10, and $a_{max} = 0.5$ meters/second.^{2} Figure 10 includes only four sets of curves (rather than five like Fig. 9) because the time required for a pure rotation of 3.14 radians ($T^2 = 2.4$) is longer than the first value for the parameter $T(T^2 = 2)$.

Sample Cartesian paths of the robot for some of these candidate time-optimal four-switch-time trajectories to a configuration are displayed (for the case where $T^2 = 10$) in Figs. 11 and 12 for final orientations of $\phi = 0.8$ radians and $\phi = 3.14$ radians, respectively. Note that, as the control trajectories evolve from Type 22−+ to 13+− to 22+−, the Cartesian trajectories change continuously.

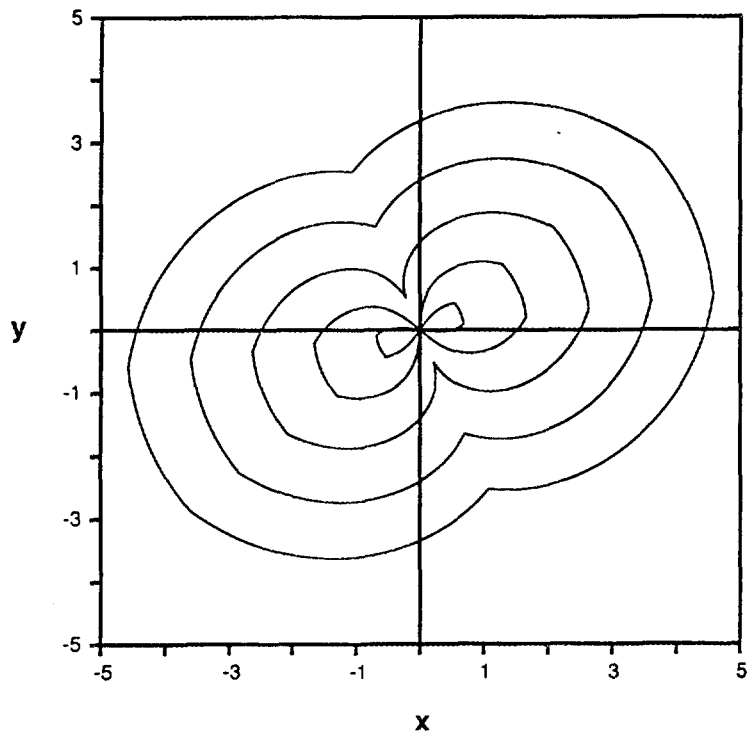

Fig. 9. Curves showing the location of the furthest points that can be reached by trajectories with four switch times for several values of $T(T^2 = 2, 4, 6, 8$, and 10) when the final orientation is 0.8 radians.

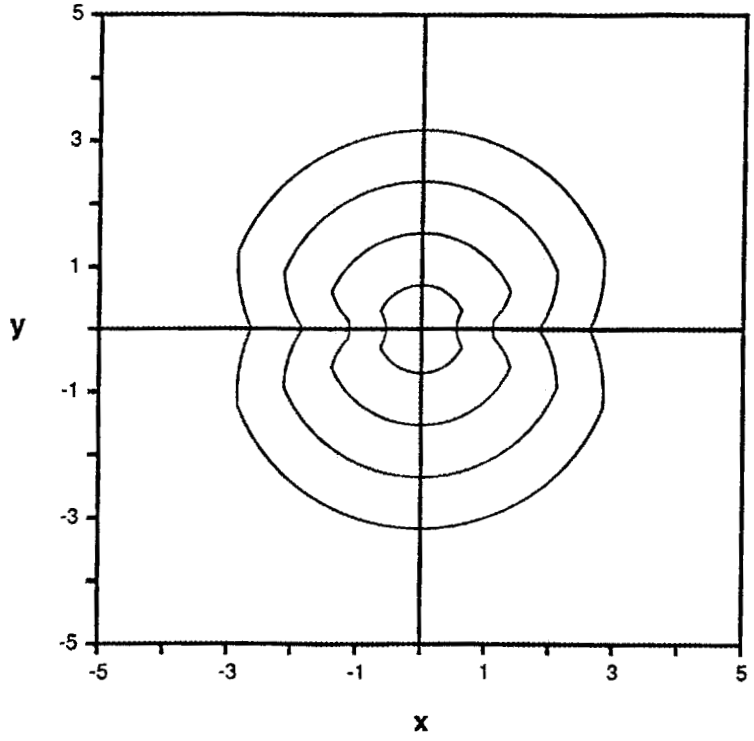

Fig. 10. Curves showing the location of points that can be reached by trajectories with four switch times for several values of $T(T^2 = 4, 6, 8,$ and $10)$ when the final orientation is 3.14 radians.

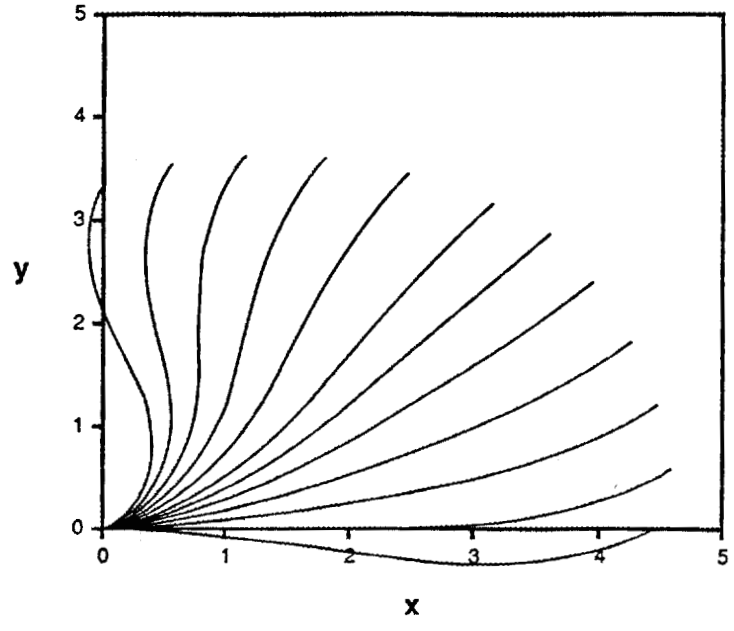

Fig. 11. Cartesian trajectories for paths with four switch times for a constant value of $T(T^2 = 10)$ when the final orientation is 0.8 radians.

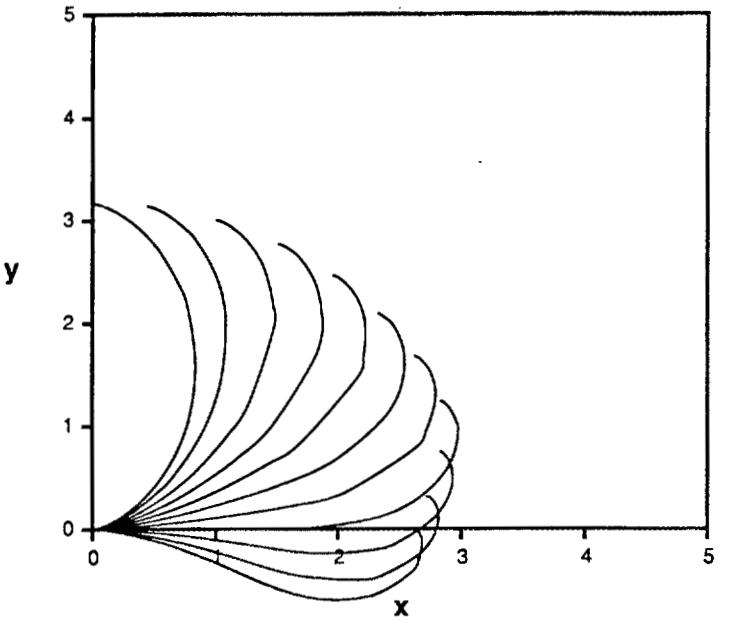

Fig. 12. Cartesian trajectories for paths with four switch times for a constant value of $T(T^2 = 10)$ when the final orientation is 3.14 radians.

6. OPTIMAL TRAJECTORIES

In this section, we show that the candidate three-switch-time trajectories identified in the previous section provide time optimal paths to a position, and the candidate four-switch-time trajectories provide time optimal paths to a configuration.

The maximum principle provides necessary (but not sufficient) conditions for an optimal trajectory. To show that a bang-bang trajectory is optimal, we must show that it satisfies the necessary conditions and that it is better than alternative paths. Indeed, we will find that some trajectories satisfy the necessary conditions but are not optimal. Since the candidate sets of trajectories have been identified through comparisons with trajectories involving the minimum needed number of switch times, we show that they are better than alternative paths by comparing them to trajectories with greater numbers of switch times.

To verify that a bang-bang trajectory satisfies the necessary conditions, we must calculate the dual variables and show that they are consistent with the control paths [that u_1 is positive (negative) when ψ_4 is positive (negative), etc.]. In Section 4, we defined four auxiliary variables (z_i) that can be used to calculate the initial conditions for the dual variables. Following the procedure described in section four, we can calculate the dual variables for any bang-bang solution.

We will consider first the three switch time trajectories to a position. Consider the results shown in Fig. 2. Our subset of candidate time-optimal-trajectories includes the trajectories of the Type 12+− that end on the first arc, i.e., the portion of the curve that lies in the first quadrant. We have calculated the dual variables for a wide range of trajectories and found that all 12+− trajectories that end on first arcs satisfy the necessary conditions. Typical results for a trajectory defined by (T, τ) = ($\sqrt{10}$, .4) are displayed in Fig. 13. The trajectory reaches the point (0.66, 4.03). For the right wheel, the acceleration is positive for (0.0 to 3.16) and negative for (3.16 to 6.32). The corresponding dual variable (ψ_4) is found positive for (0.0 to 3.16) and negative for (3.16 to 6.32). For the left wheel, the acceleration is negative for (0.0 to 0.40), positive for (0.40 to 3.56) and negative for (3.56 to 6.32). The corresponding dual variable (ψ_5) is found negative for (0.0 to 0.40), positive for (0.40 to 3.56) and negative for (3.56 to 6.32). Finally, the transversality condition requiring that $\psi_3 = 0.0$ at the end of the trajectory is seen to be verified.

We have also calculated the dual variables for the other 12+− trajectories, and it is interesting to note that they, too, satisfy the necessary conditions except for those that reach points on the spiral after it reenters the first quadrant (and the 12+− trajectories cross the 12++ trajectories). On the other hand, none of the 12++ trajectories satisfy the necessary conditions.

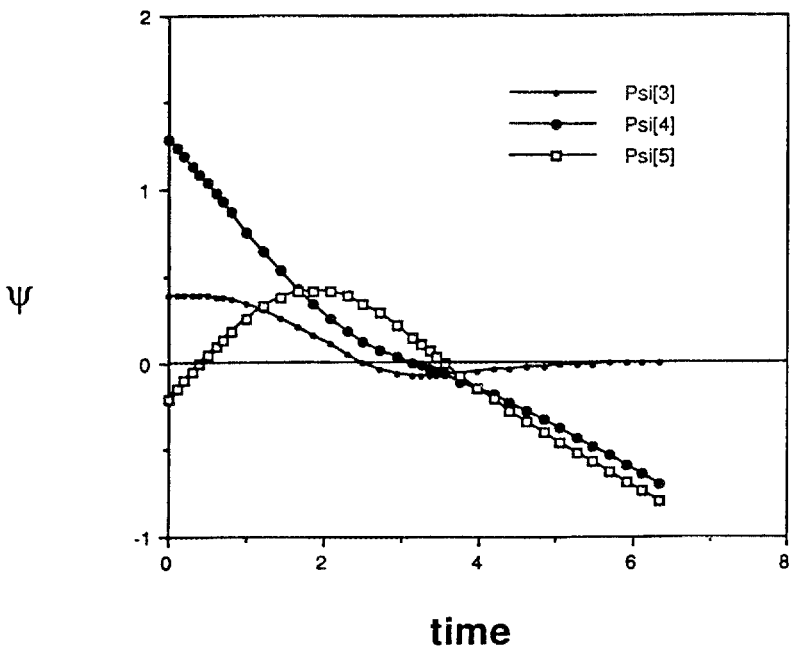

Fig. 13. Dual variables for a three-switch-time trajectory leading to the point (0.66, 4.03).

In a similar fashion, we have calculated the dual variables for a wide range of candidate time-optimal trajectories to a configuration, i.e., those four-switch-time trajectories that end at a configuration laying on $CDHEFG$ envelops of the type shown in Fig. 6, and have found that they satisfy the PMP necessary conditions. Typical results are displayed in Fig. 14 for a 22+− trajectory corresponding to $\phi = 0.8$ radians, $T^2 = 10$ and $\tau_1 = 2.84$. The trajectory reaches the configuration $(x, y, \phi) = (0.20,\ 3.43,\ 0.8)$. For the right wheel, the acceleration is positive for (0.0 to 2.84), negative for (2.84 to 6.00), and positive for (6.00 to 6.32). The corresponding dual variable (ψ_4) is found respectively positive, negative, and positive on the same interval. For the left wheel, the acceleration is negative for (0.0 to 0.52), positive for (0.52 to 3.68) and negative for (3.68 to 6.32), and the corresponding dual variable (ψ_5) is found appropriately negative, positive, and negative on the same intervals.

In the remainder of this section, we numerically demonstrate that the trajectories of the candidate sets are time-optimal by showing that they are faster than trajectories with more switch times. If the total trajectory time (T) is fixed, an optimal trajectory will reach further from the origin than any other trajectory. We demonstrate numerically that the "best" trajectories with n switch times are longer than the "best" trajectories with $n + 1$ switch times.

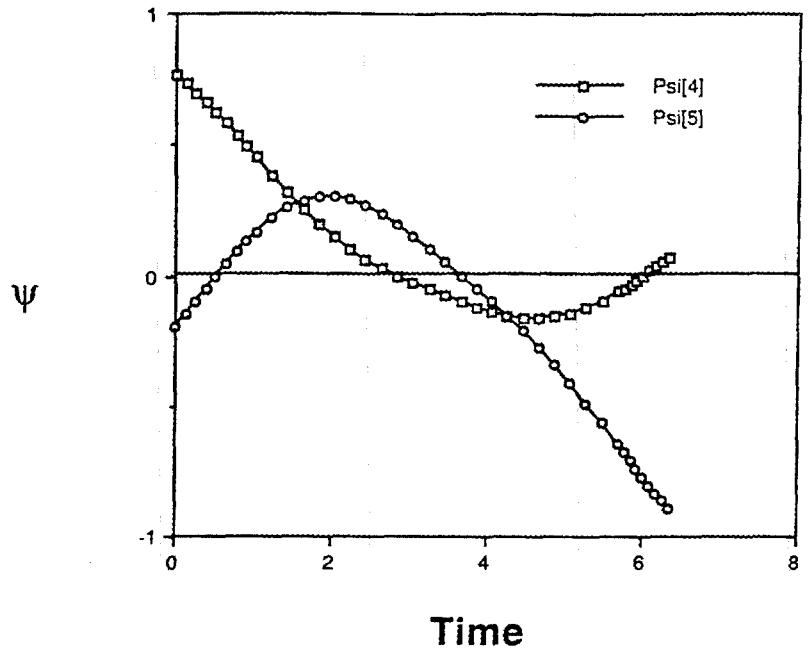

Fig. 14. Dual variables for a four-switch-time trajectory leading to the configuration (0.20, 3.43, 0.80).

A trajectory with a total of n switch times ($n_R \geq 1$ on the right wheel, $n_L \geq 1$ on the left wheel, $n_R + n_L = n$) involves $n+2$ time segments, τ_i, which are distributed on the two wheels with at least two segments on each wheel. Any n-switch-time trajectory (with $n+2$ segments) of type $n_R n_L$ can be considered as an $n+1$-switch-time trajectory (with $n+3$ segments) of type $(n_R+1)n_L$ or type $n_R(n_L+1)$ in which the additional time segment is set to zero. If we denote this additional time segment by ρ and use it as an additional trajectory parameter that can vary over its entire feasible range within $[0, \mathrm{T}]$, then all $n+1$-switch-time trajectories can be evolved from their parent n-switch-time trajectory. These can then be compared to ascertain that the parent trajectories always reach further than their "offspring" for a same total trajectory time.

First consider the special case when $n = 2$. The "best" trajectories with two switch times are pure translation (as opposed to the pure rotation trajectories which do not leave the origin). These trajectories are part of the candidate sets, although they only reach points on the x axis. However, it is clear from Fig. 2 that when the parameter is varied, the two-switch-time trajectories reach further than any three-switch-time trajectories (or trajectories with any greater number of switch times) that end on the x axis. Thus, to reach points on the x axis, these two-switch-time trajectories clearly are the time-optimal ones.

Consider the case when $n = 3$. The three switch trajectories in Fig. 2 have one switch time on the right wheel and two switch times for the left wheel, i.e., they are of Type 12. They have two types of offspring trajectories which are the only two types of four-switch-time trajectories: Type 22 and Type 13. In this case, the parameter ρ becomes either the third time segment on the right wheel or the fourth time segment on the left wheel. When the parameter is zero, the four-switch-time trajectories reduce to the three-switch-time trajectories. As the parameter increases, the offspring trajectories spanned the space of four-switch-time trajectories.

Offspring four-switch-time trajectories are compared to the parent three-switch-time trajectories in Fig. 15, for Type 22, and Fig. 16 for Type 13. In both cases, results for the parameter increasing from 0.0 to 0.3 are displayed. As the parameter increases, the end points of the four-switch-time trajectories move monotonically toward the origin. Thus, the best three-switch-time trajectories always reach further from the origin than the best four-switch-time trajectories and the distance between the end points increases as the four switch paths become less like the three switch paths.

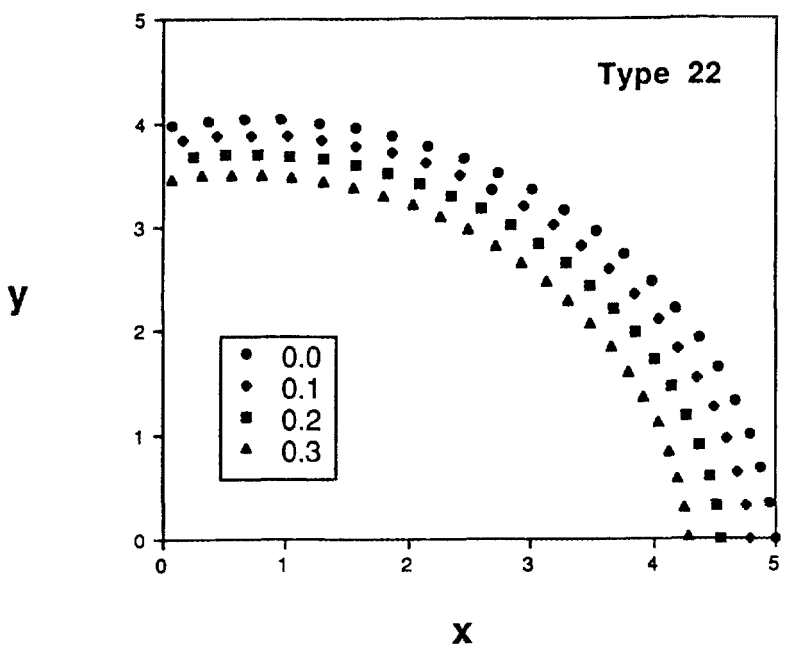

Fig. 15. Comparison of four-switch time trajectories of Type 22 and three-switch-time trajectories.

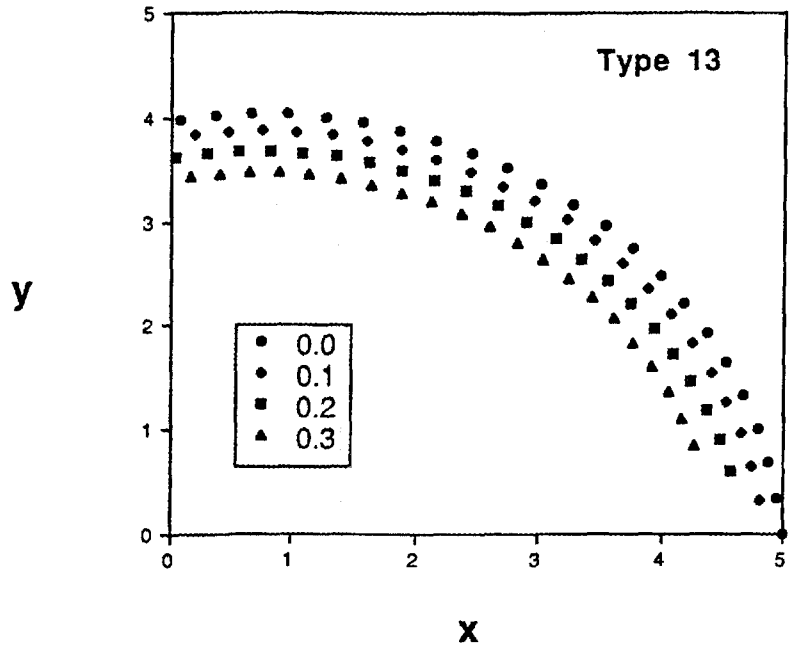

Fig. 16. Comparison of four-switch-time trajectories of Type 13 and three-switch-time trajectories.

Consider the case when $n = 4$. There are four types of five-switch-time trajectories: Type 14, Type 23, Type 32, and Type 41, which can all be found from the parents four-switch-time trajectories of Type 13 and 22, and compared to them to show that they are not time optimal. Examples of the comparison results are illustrated in Figs. 17 to 21. The Type 23+− trajectories are compared to the Type 22+− trajectories in Fig. 17. As the parameter increases from 0.0 to 0.3, the end points of the Type 23+− trajectories in the upper half plane move monotonically toward the origin. They also move toward the x axis in the first quadrant, but they always remain inside the Type 13+− and Type 22++ curves.

The Type 23+− trajectories are compared to the Type 13+− trajectories in Fig. 18. As the parameter increases from 0.0 to 0.3, the Type 23+− trajectories move monotonically toward the origin. They also move radially but they always remain inside the Type 22+− and Type 22++ curves.

The Type 23++ trajectories are compared to the Type 13++ trajectories in Fig. 19. As the parameter increases from 0.0 to 0.3, the end points of the Type 23++ trajectories move monotonically toward the origin. They also move radially but they always remain inside the Type 22+− and Type 22++ curves.

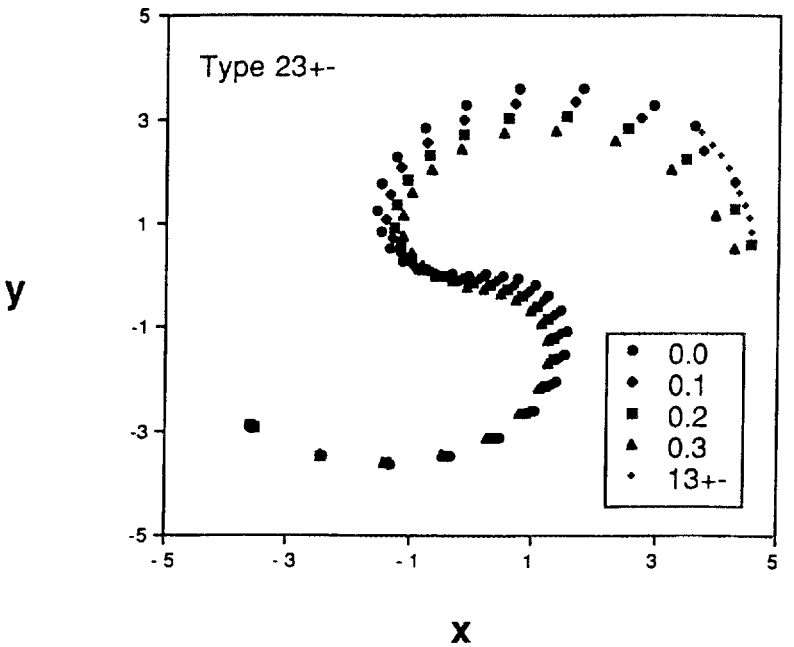

Fig. 17. Comparison of five-switch-time trajectories of Type 23+− and four-switch-time trajectories of Type 22+−.

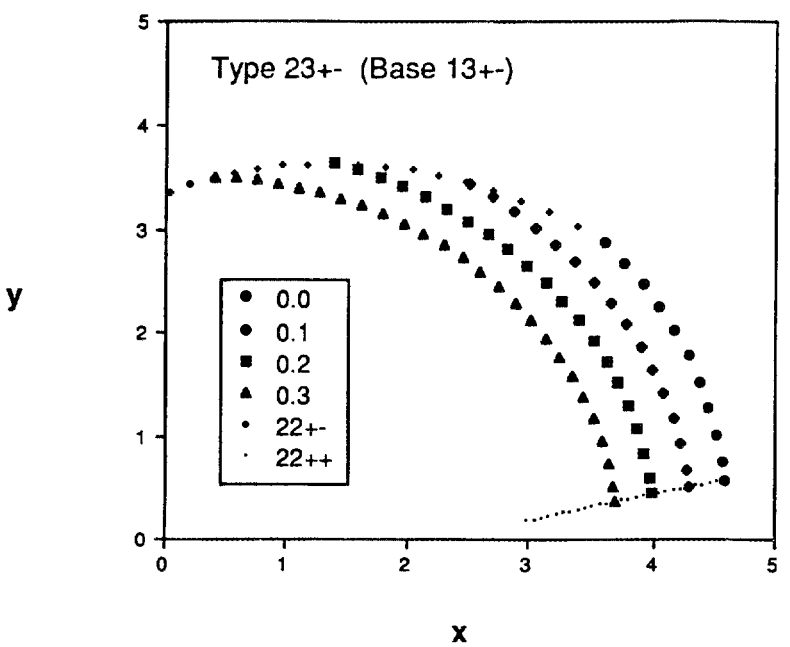

Fig. 18. Comparison of five-switch-time trajectories of Type 23+− and four-switch-time trajectories of Type 13+−.

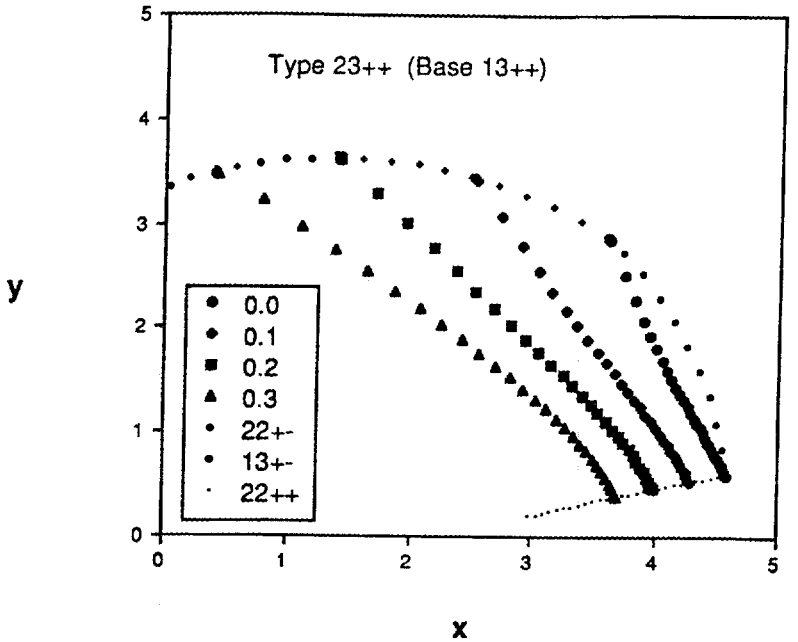

Fig. 19. Comparison of five-switch-time trajectories of Type 23++ and four-switch-time trajectories of Type 13++.

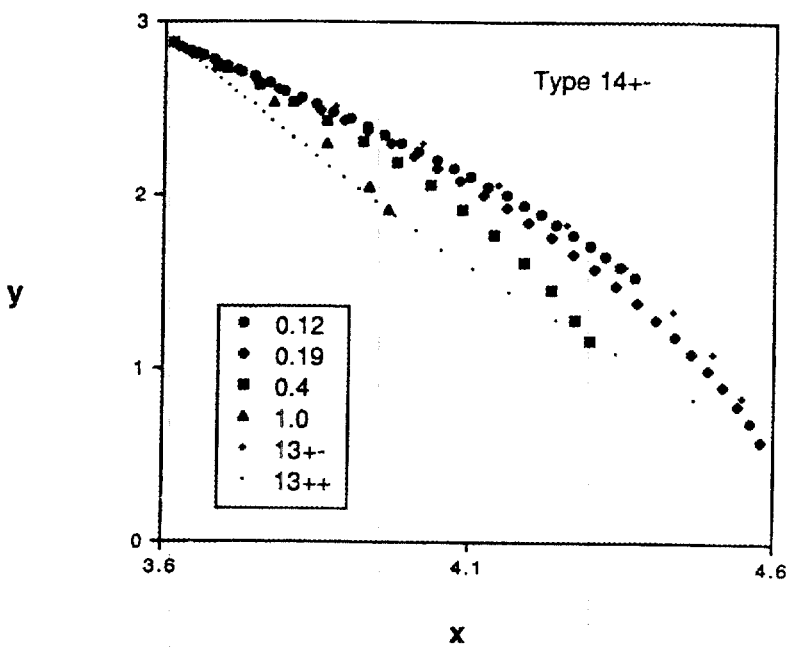

Fig. 20. Comparison of five-switch-time trajectories of Type 14+− and four-switch-time trajectories of Type 13.

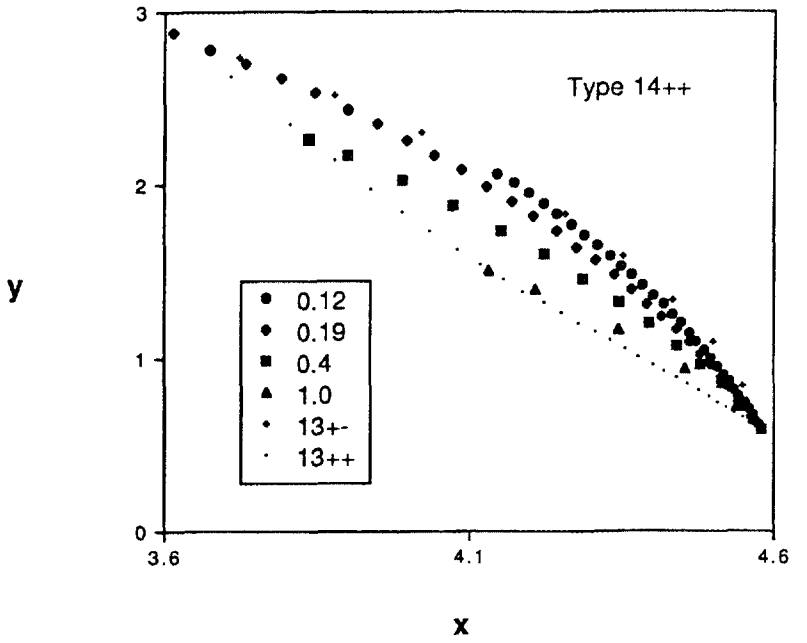

Fig. 21. Comparison of five-switch-time trajectories of Type 14++ and four-switch-time trajectories of Type 13.

The Type 14+− and Type 14++ trajectories are compared to the Type 13+− and Type 13++ trajectories in Figs. 20 and 21. The end points of the Type 14 trajectories occupy the inside of the lens shaped region defined by the Type 13 trajectories. As the parameter increases from 0 to 1.0, the end points of the Type 14 trajectories sweep the interior of the lens with a upper left fixed point for the case of Fig. 20, and a lower right fixed point for the case of Fig. 21.

Similar families of curve can be easily generated to compare parents and offspring trajectories with five switch times and greater. The important general result of such an exercise is that the best offspring trajectories never reach further than their parent best candidate for a same allowed total trajectory time.

In summary, any point in the plane can be reached by a three-switch-time trajectory which has been uniquely defined in Section 5.1 and shown to be time-optimal by reaching the desired (x, y) position faster than other three-switch-time trajectories or trajectories with a higher number of switch times. Similarly, any configuration in the plane can be reached by a four-switch-time trajectory which has been uniquely defined in Section 5.2 and shown to be time-optimal by reaching the configuration faster than other four-switch-time trajectories or trajectories with a greater number of switch times.

7. USE OF THE METHOD FOR ROBOT TRAJECTORY PLANNING

Given the results of the previous sections, the implementation on our robots has focussed on developing the driver module for the robots, i.e., the module which determines the control trajectories necessary for a time optimal motion of the platform between given subgoals in a sequence provided by the route planning module [e.g., see Vasseur, Pin and Taylor (1992) or Andersen et al. (1992)]. Each subgoal is specified as a given configuration where the platform must stop for the robot to perform some sensing, manipulation, or other tasks. In the first step of the algorithm, the arrival configuration is expressed as a relative position and orientation with respect to the starting configuration. If a final orientation is not specified, then the time-optimal three-switch-time trajectory to a point is sought which, as explained in Section 5.1, is characterized by two parameters. If a desired final orientation is specified, the time-optimal trajectory is a four-switch-time trajectory to a configuration and, as discussed in Section 5.2, Eq. (40) is first used to reduce the number of unknown parameters from three to two. In both cases, the same numerical search technique [Powell's method (Press (1988))], can thus be used to determine the two parameters (T, τ) for the given final location (x, y) making use of the symmetries with respect to the x and y axes or $\phi/2$ and $(\pi + \phi/2)$ axes as appropriate. From (T, τ) the switch times are easily calculated and the controls directly sent to the robot actuator servos.

As an example of the gain obtained with the time-optimal trajectories compared with minimum-length paths to a configuration (i.e., rotate, translate, rotate), Table 1 shows the total trajectory times required to reach the point (3,3) at several orientations. T_{opt} represents the optimal trajectory time, while T_{rtr} is the time required to execute the RTR (rotate, translate, rotate) strategy with bang-bang controls. As the orientation increases from 0.80 to 3.14 radians, T_{opt} increases from 6.18 seconds to 7.15 seconds and the ratio, $R = \mathrm{T}_{opt}/\mathrm{T}_{rtr}$, varies from .81 to .71. These results are typical of the gains obtained with optimal paths over RTR paths, and average about 25% for trajectories to near configurations (less than 5 meters away from the start point). The gain, of course, decreases as the distance separating the two configurations increases, as well as for trajectories approaching pure translations on the x axis (for which $R = 1$).

One of the concerns which usually arises when implementing time-optimal controls on a robot relates to the capability of the controller to closely approximate the bang-bang demands on the controls. For our 2,000 lbs. HERMIES-III robot, the results of well-tuned conventional PID wheel controllers (see Reister, 1992) proved extremely satisfactory, as illustrated in Fig. 22. In the figure, the velocity target on one of the wheels and the actual velocity profile obtained during experiments with the robot are displayed by the plain and dotted lines, respectively. The velocity target is a three-switch-time trajectory of the wheel with a value of $a_{\max} = .2$ m/sec^2. With this very good behavior of the controller, time-optimal motions of the robot were realized with much less than 1% error.

Table 1. Values of the optimal time (T_{opt}), the time for rotate-translate-rotate (T_{rtr}) with bang-bang controls, and their ratio (R) for paths that reach the configuration (3,3,ϕ).

ϕ Radians	T_{opt} Seconds	T_{rtr} Seconds	R
0.80	6.18	7.59	.81
1.57	6.36	8.92	.71
3.14	7.15	10.06	.71

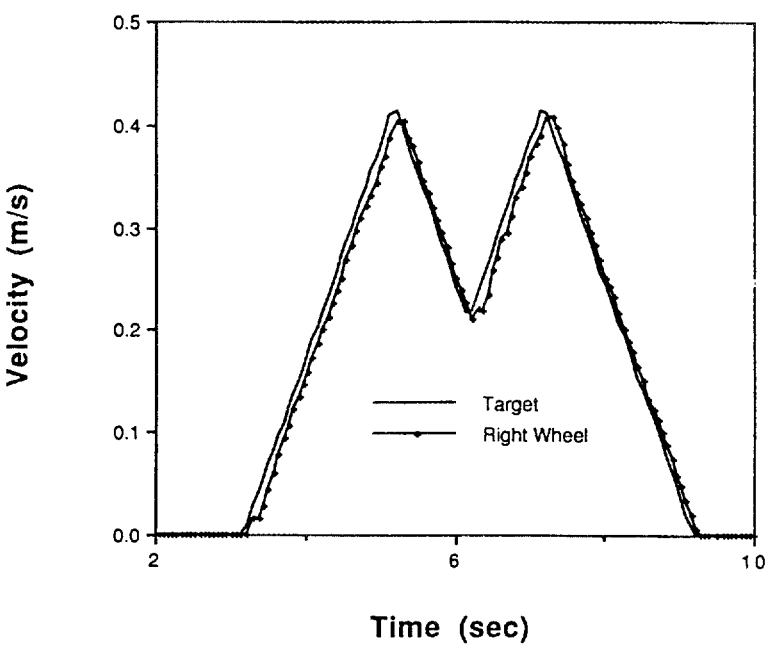

Fig. 22. Measured velocity profile for the HERMIES-III robot as it follows a bang-bang velocity target.

8. CONCLUSIONS

Our objective has been to plan time-optimal motions for a mobile robot with two independently-driven non-steerable wheels from one static configuration to the next in an unobstructed planar environment. We have used Pontryagin's Maximum Principle to prove that, when the maximum acceleration on each wheel is bounded, all optimal trajectories are bang-bang. Using this result, we have proposed a parameterization of the bang-bang trajectories which allows us to span the space of trajectories and to show that any position in the plane can be reached by a path with three switch times while any configuration can be reached by a path with four switch times. With these results, we have identified two uniquely defined subsets of paths as candidates for time-optimality.

We have then followed a numerical procedure to verify that the paths in these subsets are the time-optimal ones: we use the unique two parameters defining each path to calculate the switch times for that path, numerically integrate the control trajectories to calculate the Cartesian paths and some auxilary variables, use the auxilary variables to calculate the initial conditions for the dual variables, numerically integrate to calculate the dual variables, and verify that the Cartesian paths are consistent with the bang-bang controls as required by the maximum principle. We then numerically showed that the paths in the subsets are time-optimal by comparing them with other possible paths with larger numbers of switch times. Being numerical, the procedure required an extensive examination of many cases; however, it has allowed us to precisely identify and parameterize the set of trajectories and associated controls that allow a robot to reach any configuration in the plane in a time-optimal fashion, a problem which had eluded many efforts to date.

With the set of time-optimal trajectories identified and parameterized, we have then discussed how the results can be utilized in conjunction with a simple search technique to implement the time-optimal controls on a mobile robot. For an illustrative value of 0.5 m/sec^2 for the bound on acceleration, comparative examples indicate that the time-optimal paths can be up to 30% faster than rotate-translate-rotate paths that use bang-bang controls.

REFERENCES

1. A. Ailon and G. Langholtz, "On the Existence of Time-Optimal Control of M Mechanical Manipulators, *Journal of Optimization Theory and Applications* **46**(1), 1–21 (1985).
2. C. S. Andersen et al., "Navigation Using Range Images on a Mobile Robot," accepted for publication in *Robotics and Autonomous Systems* (1992).
3. R. C. Arkin, "Integrating Behavioral, Perceptual, and World Knowledge in Reactive Navigation," *Robotics and Autonomous Systems* **6**(1 & 2), 105–122 (1990).
4. G. L. Blaisdell, "Performance of an Omnidirectional Wheel on Snow and Ice," *Naval Engineers Journal* **103**(1), 34–41 (1991).
5. J. E. Bobrow, "Optimal Robot Path Planning Using the Minimum-Time Criterion," *IEEE J. of Robotics and Automation* **4**(4), 443–450 (1988).
6. R. A. Brooks, "Elephants Don't Play Chess," *Robotics and Autonomous Systems* **6**(1 & 2), 3–15 (1990).
7. Y. Chen and A. A. Desrochers, "A Proof of the Structure of the Minimum-Time Control Law of Robotic Manipulators Using a Hamiltonian Formulation," *IEEE Transactions on Robotics and Automation* **6**(3), 388–393 (1990).
8. A. M. Formal'skii and S. N. Osipov, "On the Problem of the Time-Optimal Manipulator Arm Turning," *IEEE Transactions on Automatic Control* **35**(6), 714–719 (1990).
9. H. P. Geering et al., "Time-Optimal Motions of Robots in Assembly Tasks," *IEEE Transactions on Automatic Control* **31**(6), 512–518 (1986).
10. G. Giralt, R. Chatila, and M. Vaisset, "An Integrated Navigation and Motion Control System for Autonomous Multisensory Mobile Robots," *Robotics Research: The First International Symposium*, M. Brady and R. P. Paul, eds., MIT Press, Cambridge, Massachusetts, 1984.
11. P. Jacobs, J. P. Laumond, and A. Rege, "Non-Holonomic Motion Planning for Hilare-Like Mobile Robots," *Proc. of the International Symposium on Intelligent Robotics*, 338–347 (1991).
12. M. E. Kahn and B. Roth, "The Near-Minimum-Time Control of Open-Loop Articulated Kinematic Chains," *ASME Journal of Dynamic Systems, Measurement, and Control* **93**(3), 164–172 (1971).
13. Y. Kanayama and B. I. Hartman, "Smooth Local Path Planning for Autonomous Vehicles," *Proc. IEEE International Conference on Robotics and Automation*, 1265–1270 (1989).
14. S. M. Killough and F. G. Pin, "A Fully Omnidirectional Wheeled Assembly for Robotic Vehicles," *Trans. Am. Nucl. Soc.* **61** 425–426 (1990).

15. B. K. Kim and K. G. Shin, "Suboptimal Control of Industrial Manipulators with a Weighted Minimum Time-Fuel Criterion," *IEEE Transactions on Automatic Control* **30**(1), 1–10 (1985).

16. Y. Koren and J. Borenstein, "Potential Field Methods and Their Inherent Limitations for Mobile Robot Navigation," *Proc. IEEE International Conference on Robotics and Automation*, 1398–1404 (1991).

17. Y. Nakamura and H. Hanafusa, "Optimal Redundancy Control of Robot Manipulators," *Int. J. Robotics Research* **6**(1), 32–42 (1987).

18. M. Niv and D. M. Auslander, "Optimal Control of a Robot with Obstacles," *Proc. of the American Control Conference*, 280–287 (1984).

19. S. N. Osipov and A. M. Formal'skii, "The Problem of the Time-Optimal Turning of a Manipulator," *Applied Mathematics and Mechanics* **52**(6), 725–731 (1988).

20. L. S. Pontryagin et al., *L. S. Pontryagin Selected Works, Volume 4: The Mathematical Theory of Optimal Processes,* Gordon and Breach Science Publishers, New York (1986).

21. W. H. Press et al., *Numerical Recipes in C: The Art of Scientific Computing*, Cambridge, UK: Cambridge University Press, 1988.

22. D. B. Reister, "A New Wheel Control System for the Omnidirectional HERMIES-III Robot," accepted for publication in *Robotica* (1992).

23. L. G. Van Willigenburg, "First Order Controllability and the Time Optimal Control Problem for Rigid Articulated Arm Robots with Friction," *Int. J. Control* **51**(6), 1159–1171 (1990).

24. H. A. Vasseur, F. G. Pin, and J. R. Taylor, "Navigation of a Car-Like Mobile Robot Using a Decomposition of the Environment in Convex Cells," *Proc. IEEE International Conference on Robotics and Automation*, 1496–1502 (1991).

25. A. Weinreb and A. E. Bryson, "Optimal Control of Systems with Hard Control Bounds," *IEEE Transactions on Automatic Control* **30**(11), 1135–1138 (1985).

26. C. R. Weisbin, G. de Saussure, J. R. Einstein, F. G. Pin, and E. Heer, "Autonomous Mobile Robot Navigation and Learning," *Computer* **22**(6), 29–35 (June 1989).

27. J. Wen, "On Minimum Time Control for Robotic Manipulators," *Recent Trends in Robotics: Modeling, Control, and Education,* North-Holland, New York, 283–292 (1986).

28. M. Yamamoto and A. Mohri, "Planning of Quasi-Minimum Time Trajectories for Robot Manipulators (Generation of a Bang-Bang Control)," *Robotica* **7**, 43–47 (1989).

INTERNAL DISTRIBUTION

1. B. R. Appleton
2. J. E. Baker
3. A. L. Bangs
4. M. Beckerman
5. B. L. Burks
6. R. J. Carter
7. J. R. Einstein
8. C. W. Glover
9. X. Guan
10. W. R. Hamel
11. J. N. Herndon
12. J. F. Jansen
13. J. P. Jones
14. H. E. Knee
15. R. L. Kress

16–20. R. C. Mann

21. E. M. Oblow

22–26. F. G. Pin

27–31. D. B. Reister

32. J. C. Schryver
33. P. F. Spelt
34. F. J. Sweeney
35. E. C. Uberbacher
36. M. A. Unseren

37–41. R. C. Ward

42. EPMD Reports Office

43–44. Laboratory Records Department

45. Laboratory Records, ORNL-RC
46. Document Reference Section
47. Central Research Library
48. ORNL Patent Section

EXTERNAL DISTRIBUTION

49. Dr. Peter Allen, Department of Computer Science, 450 Computer Science, Columbia University, New York, NY 10027
50. Mr. Harry Alter, Division of Advanced Technology Development, U.S. Department of Energy, Washington, DC 20545
51. Dr. John Baillieul, Aerospace and Mechanical Engineering Department, Boston University, 110 Cummington St., Boston, MA 02215
52. Dr. Wayne Book, Department of Mechanical Engineering, J. S. Coon Building, Room 306, Georgia Institute of Technology, Atlanta, GA 30332
53. Dr. Johann Borenstein, The University of Michigan, 1101 Beal Ave., Ann Arbor, MI 48109-2110
54. Professor Roger W. Brockett, Wang Professor of Electrical Engineering and Computer Science, Division of Applied Sciences, Harvard University, Cambridge, MA 02138
55. Professor Carl Crane, 202 Nuclear Science Center, University of Florida, Gainesville, FL 32611
56. Professor John J. Dorning, Department of Nuclear Engineering and Physics, Thornton Hall, McCormick Rd., University of Virginia, Charlottesville, VA 22901
57. Dr. Steven Dubowsky, Massachusetts Institute of Technology, Building 3, Room 469A, 77 Massachusetts Ave., Cambridge, MA 02139
58. Dr. Ralph C. Gonzalez, Department of Electrical and Computer Engineering, The University of Tennessee, Knoxville, TN 37996-2100
59. Dr. Avi Kak, Department of Electrical Engineering, Purdue University, Northwestern Ave., Engineering Mall, Lafayette, IN 47907
60. Professor Takeo Kanade, Computer Science and Robotics, Carnegie Mellon University, Pittsburgh, PA 15213-3890
61. Dr. James E. Leiss, 13013 Chestnut Oak Dr., Gaithersburg, MD 20878

61. Professor Suzanne M. Lenhart, Department of Mathematics, The University of Tennessee, 304 Ayres Hall, Knoxville, TN 37996-1300
62. Dr. Oscar P. Manley, Division of Engineering, Mathematical, and Geosciences, Office of Basic Energy Sciences, ER-15, U.S. Department of Energy - Germantown, Washington, DC 20545
63. Professor Neville Moray, Department of Mechanical and Industrial Engineering, University of Illinois, 1206 West Green St., Urbana, IL 61801
64. Dr. Shankar Shastry, Department of EECS, 261-M Cory Hall, University of California, Berkeley, CA 94720
65. Dr. Wes Snyder, Center for Communications and Signal Processing, North Carolina State University, P.O. Box 7914, Raleigh, NC 27695-7914
66. Professor Delbert Tesar, Department of Mechanical Engineering, 26 San Jacinto, University of Texas, Austin, TX 78712
67. Professor M. A. Trivedi, Department of Electrical and Computer Engineering, The University of Tennessee, Knoxville, TN 37996-2100
68. Professor James S. Tulenko, 202 Nuclear Science Center, University of Florida, Gainesville, FL 32611
69. Professor David K. Wehe, Department of Nuclear Engineering, 2355 Bonisteel Blvd., The University of Michigan, Ann Arbor, MI 48109-2106
70. Professor Mary F. Wheeler, Department of Mathematical Sciences, Rice University, P.O. Box 1892, Houston, TX 77251
71. Office of Assistant Manager for Energy Research and Development, U.S. Department of Energy, Oak Ridge Operations Office, P.O. Box 2001, Oak Ridge, TN 37831-8600

72–81. Office of Scientific Technical Information, P.O. Box 62, Oak Ridge, TN 37831